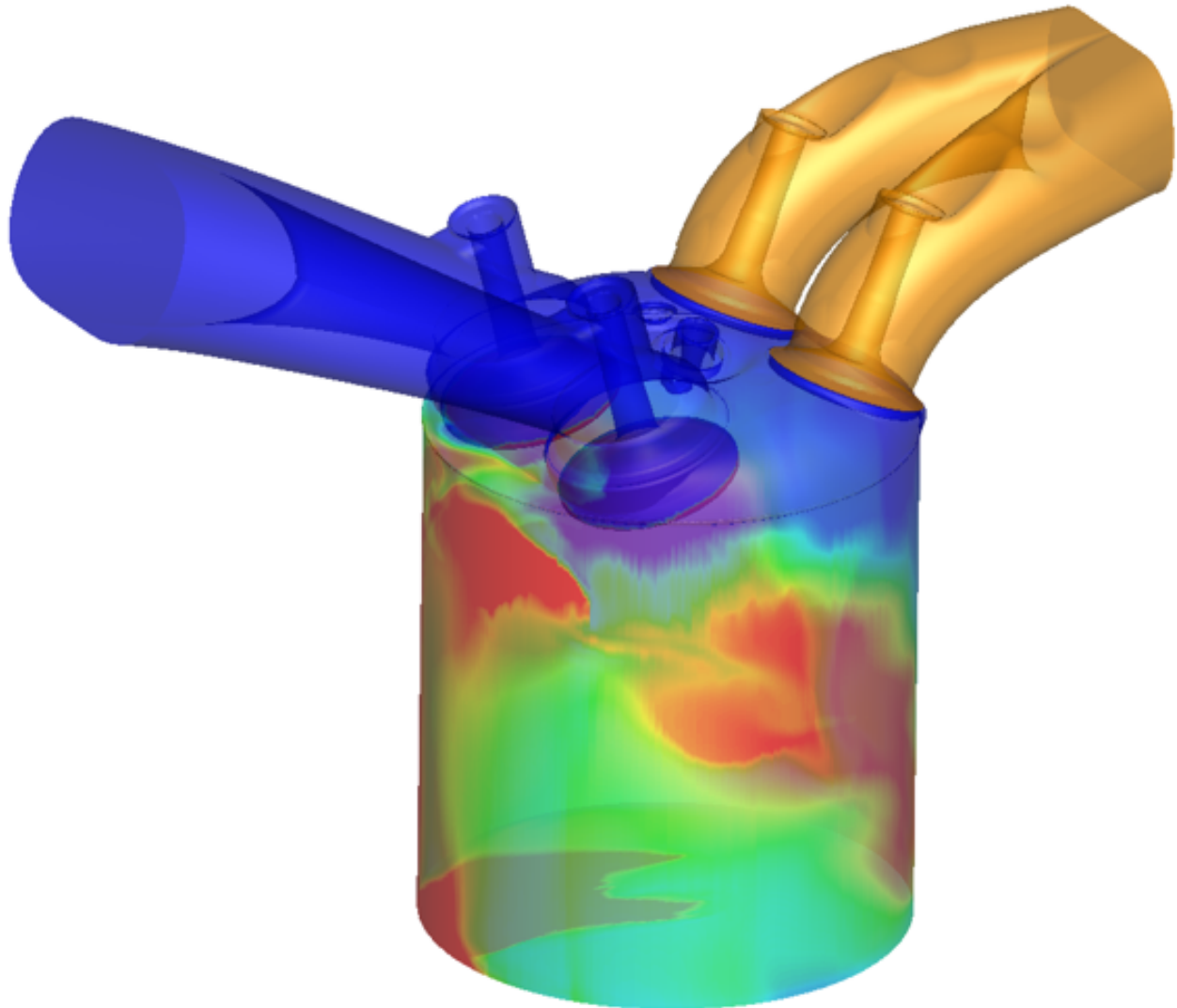




**CHALMERS**  
UNIVERSITY OF TECHNOLOGY



# **CFD simulations of mixing processes in Direct Injection SI engines**

Master's thesis in Automotive Engineering - MPAUT

Nithin Revadal  
Subhash Ravi Kumar

---

**DEPARTMENT OF MECHANICS AND MARITIME SCIENCES**

CHALMERS UNIVERSITY OF TECHNOLOGY

Gothenburg, Sweden 2021

[www.chalmers.se](http://www.chalmers.se)



MASTER'S THESIS IN AUTOMOTIVE ENGINEERING 2021

# CFD simulations of mixing processes in Direct Injection SI engines

Nithin Revadal  
Subhash Ravi Kumar



Department of Mechanics and Maritime Sciences  
*Division of Combustion and Propulsion Systems*  
CHALMERS UNIVERSITY OF TECHNOLOGY  
Gothenburg, Sweden 2021

CFD simulations of mixing processes in Direct Injection SI engines

© Nithin Revadal, Subhash Ravi Kumar, 2021.

Supervisor and Examiner: Petter Dahlander  
Professor at division of Combustion and Propulsion Systems  
Mechanics and Maritime Sciences, Chalmers University of Technology

Master's Thesis 2021  
Department of Mechanics and Maritime Sciences  
Division of Combustion and Propulsion systems  
Chalmers University of Technology  
SE-412 96 Gothenburg  
Telephone +46 31 772 1000

Cover: Equivalence ratio of iso-octane at -180CAD, obtained from Tecplot for CON-  
VERGE.

Typeset in L<sup>A</sup>T<sub>E</sub>X  
Printed by Chalmers Reproservice  
Gothenburg, Sweden 2021

# Abstract

To keep up with stringent emission standards and Internal Combustion Engines (ICE) having major market share of all the motor vehicles in the world, it is necessary to explore the avenues to decrease emissions and improve efficiency of the ICE engines.

In this thesis the effects of varying piston and fuel temperatures on mixing process and fuel film mass on the piston surface were studied using CONVERGE CFD software. The simulations were performed by selecting a single component (iso-octane) and a multi-component fuel blend (iso-octane, n-hexane, n-decane) as surrogates for gasoline, in a Volvo single cylinder medium tumble 4 valve direct injection engine. Simulations were performed with piston temperatures of 380K, 430K, 450K and with fuel temperatures 335K and 363K.

The piston temperature played an important role in the quality of mixing, as the higher piston temperature led to faster vaporisation, better mixing. Whereas lower piston temperature caused leaner mixture as some the fuel failed to vaporise. A higher fuel temperature resulted in better mixing with single component fuel, whereas with multi-component fuel and its wide boiling temperature range showed poorer mixing.

Keywords: Internal combustion engines, CFD, simulation, mixing, fuel film mass.



# Acknowledgements

First and foremost we would like to offer our sincere gratitude to Petter Dahlander, who guided us in every step and provided his valuable time for this thesis. Without which, finishing this thesis would have been impossible.

We would also like to thank the PhD and Postdoc researchers, Sreelekha Etikyala and Rafig Babayev in the Combustion and Propulsion Systems division, for their diligent efforts in answering our many questions.

Convergent Science provided CONVERGE licenses and technical support for this work.

We are eternally grateful for our family for their continuous support and, never ending love and belief in us.

Gothenburg, June 2021

Nithin Revadal and Subhash Ravi Kumar





# Contents

<b>List of Figures</b>	<b>xi</b>
<b>List of Tables</b>	<b>xiii</b>
<b>1 Introduction</b>	<b>1</b>
1.1 Aim and Objective . . . . .	1
1.2 Background work . . . . .	2
1.3 Fixing the geometric defects . . . . .	4
1.3.1 Intersecting Triangles . . . . .	4
1.3.2 Non-Manifold Edges . . . . .	5
1.3.3 Open Edges . . . . .	5
1.3.4 Normal Orientation . . . . .	5
1.3.5 Isolated Triangles . . . . .	5
<b>2 Method</b>	<b>7</b>
2.1 Case setup . . . . .	7
2.1.1 Boundary conditions . . . . .	8
2.1.2 Spray modeling . . . . .	10
2.1.3 Drop evaporation . . . . .	11
2.1.4 Drop wall interaction . . . . .	12
2.1.4.1 Wall film model . . . . .	12
2.1.4.2 Drop/Film rebound . . . . .	12
2.1.4.3 Drop/film splashing . . . . .	12
2.1.5 Spray breakup . . . . .	13
2.1.5.1 Kelvin-Helmholtz model . . . . .	14
2.1.5.2 Rayleigh-Taylor model . . . . .	14
2.1.6 Regions and Initialization . . . . .	15
2.1.7 Events . . . . .	16
2.1.8 Grid control . . . . .	16
2.1.8.1 Fixed Embedding . . . . .	17
2.1.8.2 Adaptive Mesh Refinement (AMR) . . . . .	18
2.2 Operating parameters . . . . .	19
2.3 Multi component fuel . . . . .	20
<b>3 Results and discussion</b>	<b>23</b>
3.1 Reverse flow into intake manifold . . . . .	23
3.1.1 Reverse flow with single component fuel . . . . .	24

3.1.2	Reverse flow with multi-component fuel . . . . .	25
3.2	Single component fuel . . . . .	28
3.2.1	Baseline simulation . . . . .	28
3.2.1.1	Pressure . . . . .	28
3.2.1.2	Fuel film mass on piston . . . . .	29
3.2.1.3	Mixing . . . . .	29
3.2.1.4	Temperature . . . . .	31
3.2.2	Fuel film mass on piston . . . . .	32
3.2.2.1	Effects of varying surface piston temperature . . . . .	32
3.2.2.2	Effects of increasing fuel temperature . . . . .	33
3.2.3	Mixing process . . . . .	34
3.2.3.1	Piston temperature = 380K . . . . .	34
3.2.3.2	Piston temperature = 450K . . . . .	35
3.2.3.3	Fuel temperature = 363K . . . . .	36
3.3	Multi component fuel . . . . .	37
3.3.1	Baseline simulation . . . . .	37
3.3.1.1	Pressure . . . . .	37
3.3.1.2	Fuel film mass on piston . . . . .	38
3.3.1.3	Mixing Process . . . . .	39
3.3.1.4	Temperature . . . . .	40
3.3.2	Fuel film mass on piston . . . . .	41
3.3.2.1	Effects of varying surface piston temperature . . . . .	41
3.3.2.2	Effects of increasing fuel temperature . . . . .	42
3.3.3	Mixing process . . . . .	43
3.3.3.1	Piston temperature = 380K . . . . .	43
3.3.3.2	Piston temperature = 450K . . . . .	44
3.3.3.3	Fuel temperature = 363K . . . . .	45
<b>4</b>	<b>Conclusion</b>	<b>47</b>
<b>5</b>	<b>Future work</b>	<b>49</b>
	<b>Bibliography</b>	<b>51</b>

# List of Figures

1.1	Intersecting triangles . . . . .	3
1.2	Open edge error . . . . .	3
1.3	Geometric defects upon running diagnosis in Converge [3] . . . . .	4
2.1	Front view of the Cylinder . . . . .	7
2.2	Top view of the Cylinder . . . . .	8
2.3	Boundary conditions [3] . . . . .	9
2.4	Possible parcel wall interaction outcomes in Kuhnke model [2]. . . . .	13
2.5	Schematic of the KH-RT spray breakup model [2] . . . . .	15
2.6	A visualisation of fixed embedding around the valve [2] . . . . .	18
2.7	Vaporisation profile [5] . . . . .	20
3.1	Reverse flow of iso-octane . . . . .	24
3.2	Fuel back flow with iso-octane . . . . .	24
3.3	Fuel back flow with iso-octane [Tw 380 vs 430K] . . . . .	25
3.4	Fuel back flow of iso-octane in MCF . . . . .	25
3.5	Fuel back flow of n-hexane in MCF . . . . .	26
3.6	Fuel back flow of n-decane in MCF . . . . .	26
3.7	Pressure inside the cylinder . . . . .	28
3.8	Fuel film mass on piston . . . . .	29
3.9	Equivalence ratio distribution with Piston temperature at 430K . . . .	30
3.10	Temperature inside the cylinder for SCF . . . . .	31
3.11	Fuel film mass on piston with varying piston temperatures . . . . .	32
3.12	Fuel film mass on piston with Fuel temperature at 363K . . . . .	33
3.13	Equivalence ratio distribution with Piston temperature at 380K . . . .	34
3.14	Equivalence ratio distribution with Piston temperature at 450K . . . .	35
3.15	Equivalence ratio distribution with Fuel temperature at 363K . . . . .	36
3.16	Pressure inside the cylinder for MCF . . . . .	37
3.17	Fuel film mass on piston for MCF with Piston temperature at 430K . .	38
3.18	Equivalence ratio distribution with Piston temperature at 430K . . . .	39
3.19	Temperature inside the cylinder for MCF . . . . .	40
3.20	Fuel film mass on piston with varying piston temperatures for MCF . .	41
3.21	Fuel film mass on piston for MCF with Fuel temperature at 363K . . .	42
3.22	Equivalence ratio distribution for MCF with Piston temperature at 380K . . . . .	43
3.23	Equivalence ratio distribution for MCF with Piston temperature at 450K . . . . .	44

3.24	Equivalence ratio distribution for MCF with Fuel temperature at 363K	45
------	--	----

# List of Tables

2.1	Engine specifications . . . . .	8
2.2	Spray modeling parameters . . . . .	10
2.3	Regions and initialisation parameter setup . . . . .	16
2.4	Boundary temperatures . . . . .	19
2.5	Simulation parameters . . . . .	19
2.6	Fuel properties of Gasoline and multi-component fuel . . . . .	20



# 1

## Introduction

With an eye on the global warming and increasing stringent emission standards, it is imperative to increase the efficiency, as well as reduce emissions of Internal Combustion Engines (ICE), who account for majority of all the motor vehicles in the world today. Computational Fluid Dynamics (CFD) simulations are an effective tool to study the behaviour of the fluids interacting with various surfaces or geometries. In the field of automotive engineering, CFD simulations are extensively employed to study the behaviour and characteristics of ICE under different operating conditions.

With its autonomous meshing, various and efficient chemistry solvers, and the ability to accommodate complex moving geometry, CONVERGE CFD software was the best option to run our simulations on. It has robust example models and an extensive user manual to understand both the user interface and the inner workings i.e. physical and chemical models employed in it.

In this thesis we implemented the geometry of a cylinder, belonging to an engine used in an experimental setup at the department of Combustion and Propulsion Systems, in Chalmers University of Technology, into the CONVERGE. This gave us an exciting opportunity to run our simulations at practical operating conditions, and to comprehend, explain the results better.

### 1.1 Aim and Objective

The principle aim of this thesis is to study the mixing processes in a Gasoline Direct Injection (GDI) spark ignition (SI) engine, along with the liquid fuel film on the piston surface. The thesis was carried out with an extensive use and exploration of the CONVERGE CFD software, which aided in implementing the geometry and interpret the results effectively.

A good mixing process is one of the significant gateways for clean combustion and better fuel efficiency of the engine. To keep up with the emission standards it is important to study the mixing process of air and vaporised fuel in an ICE, as it contributes to the better extrapolation of parameters affecting the combustion and thus the emissions.

The objectives of the thesis are listed below,

- Implement the geometry of the cylinder from experimental setup into the simulation software.
- Simulate by introducing a single component and multi-component fuel, as surrogates for the gasoline into the setup.
- Running simulations on different scenarios, by altering the initial operating conditions of the case setup through,
  - Varying the temperature of the piston.
  - Increasing the fuel temperature.

## 1.2 Background work

As the aim of the thesis is to study the fuel film mass on piston surface and mixing process at the end of compression stroke under different parameters, an extensive literature survey was conducted to understand the causes and results better.

CONVERGE CFD being relatively new to the department of Combustion and Propulsion Systems, posed a few challenges when implementing a new geometry into the software. To implement the new Computer-aided design (CAD) geometry, a STL file generated from a CAD software was initially introduced into the Converge environment using a python script.

Once the CAD geometry was successfully imported into CONVERGE CFD, the software automatically meshes the geometry assessing the different boundaries present. But, it contains numerous geometric defects which needs to be rectified. The most commonly encountered geometric defects are:

1. Intersecting triangles.
2. Non-manifold edges.
3. Open edges.
4. Normal orientation inconsistencies.
5. Isolated triangles.

1. **Intersecting triangles:** Intersecting triangles essentially means that two are more triangles are traversing through each other in the present geometry. It must be noted that, even if the error does not exist at one time frame in the geometry, it could appear when the motion is assigned to the geometry that is being simulated which could lead to fatal error of the simulation. Figure [1.1] shows a two dimensional example.



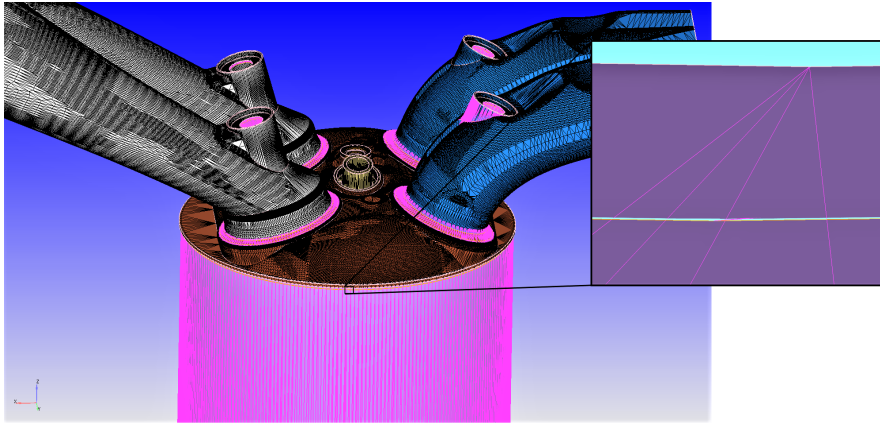


**Figure 1.1:** Intersecting triangles

2. **Non-manifold edges:** Any edge of an element must connect two triangles to it. Non-manifold error occurs when an edge is shared by more than two triangles to it.
3. **Open edges:** Open edge defects occur when at least one of the triangles of the geometry does not have an adjoining triangle on each of its edges.

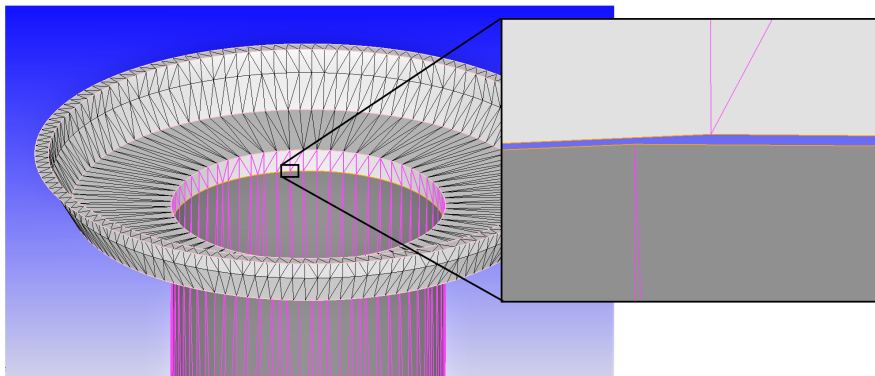


**Figure 1.2:** Open edge error

4. **Normal orientation inconsistencies:** Normal Orientation inconsistency occurs when all the connected triangles' normal vectors of a boundary are not pointing towards one of the two directions (axially inwards or outwards). This helps define which surface interacts with the fluid and the surface that does not come in contact with the fluid.  
It is preferred to have the normal vector of all the triangles pointing in the direction where the fluid flows
5. **Isolated triangles:** Isolated Triangle defect occurs when a triangle does not share any of its three edges with the adjoining triangle of the same boundary, essentially encompassed by triangles of a different boundary on all sides.

Upon running diagnostics for the first time following surface defects were encountered,

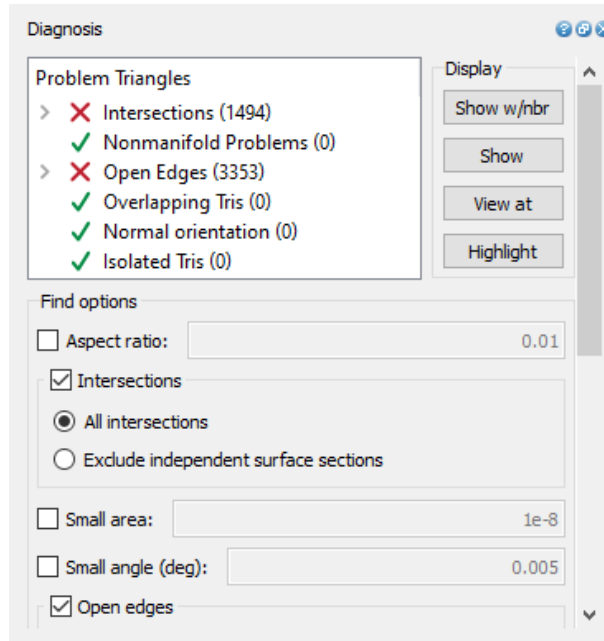


**Figure 1.3:** Geometric defects upon running diagnosis in Converge [3]

## 1.3 Fixing the geometric defects

Rectifying the above defects becomes simpler when clearly defined Boundary lines and Boundary fences are present.

- **Boundary Line :** The line consisting of edges which connects two adjacent boundaries.
- **Boundary Fence :** The line consisting of edges marking clear distinction between start/end of a complex geometric shape in a boundary.

### 1.3.1 Intersecting Triangles

- **Delete and Re-create:** One or an array of triangles intersecting are deleted and new triangles are created in it's place. If a clear boundary line/fence is defined, these triangles are assigned to their respective boundaries automatically.
- **Re-Align and Stitch :** If the boundary lines/fence of the array of triangles intersecting each other are clearly defined. Re-aligning them to the required axis and stitching the boundary lines together is the quick and easy way to fix the issue.

### 1.3.2 Non-Manifold Edges

Non-Manifold edge surface defects are comparatively a rare occurrence. But when it appears, it is usually a singled-out element.

- **Delete and Re-create :** The element whose edge is connected to more than two triangle is to be deleted and two or more triangles need to be created in its place, so that further non-manifold errors are not shown.

### 1.3.3 Open Edges

- **Patch:** This solution is used to close an open surface when there is a clear boundary fence present, around the missing triangles.
- **Create:** If the boundary fences are not clearly defined, they are defined manually. Then triangles are created at required positions and assigned to corresponding boundary.

### 1.3.4 Normal Orientation

- **Attempt to fix all normal:** In CONVERGE studio, Transform > Normal > Attempt to fix all normals is the best fix, where the software automatically recognizes and fixes all the normal orientation defects of the geometry.
- **Manually change normal:** If the above method does not work, the normals of individual triangle or the triangles of a boundary are changed under Transform > Normal > Propagate change for single triangle/Reverse all normals in a boundary.

### 1.3.5 Isolated Triangles

- **Select individual triangle and assign :** If there are very few isolated triangles, they are individually selected and assigned to the corresponding boundary.
- **Select boundary and assign :** If there are numerous isolated triangles inside a boundary. All the triangles of that boundary are selected and assigned to the corresponding boundary instead of selecting the triangles individually.



# 2

## Method

### 2.1 Case setup

The geometry selected for this simulation was a Volvo single cylinder medium tumble 4 valve direct injection engine. The major reason for choosing this engine was its relevance in today's market and the availability of data i.e. an experimental setup with the same engine is used in the department of Combustion and propulsion Systems at Chalmers University of Technology. Hence obtaining realistic data for the simulations, which usually is a difficult and time consuming task, was effortless in this case and thus helped in the better time management of the project.

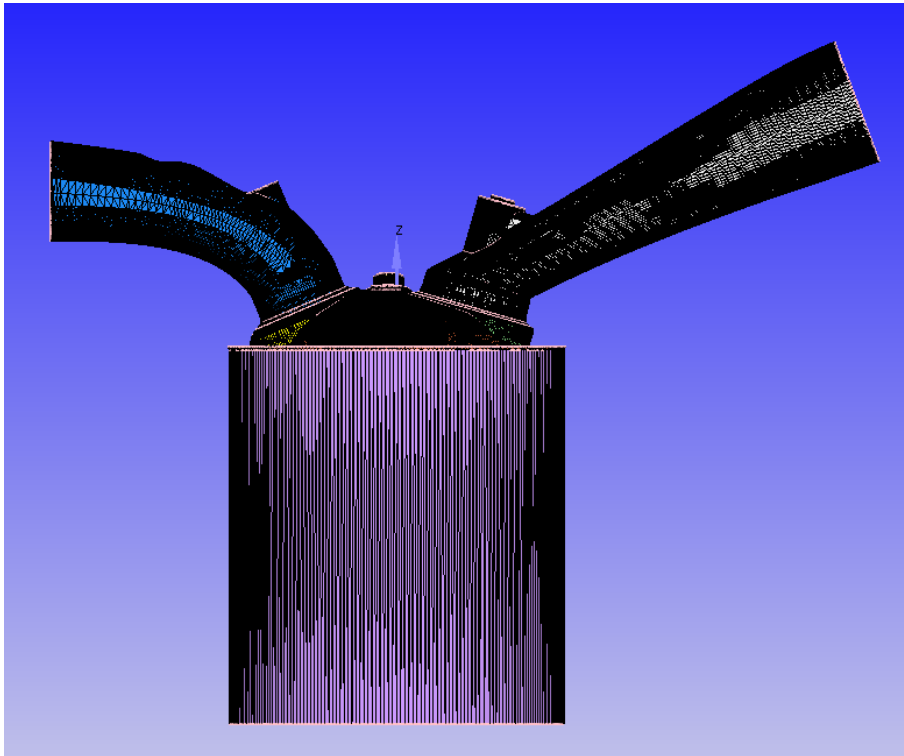


**Figure 2.1:** Front view of the Cylinder

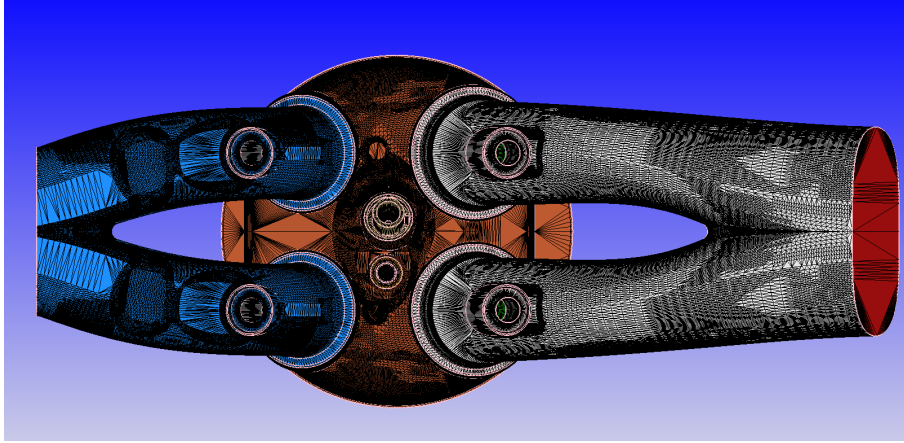


**Figure 2.2:** Top view of the Cylinder

The specifications of the selected single cylinder engine,

Cylinder volume	475cc
Bore	82mm
Stroke	90mm
Engine head	4 valve SGDI
Spark plug	Single electrode
Injector type	6 hole solenoid
Injection pressure	$\approx 200$ bar
Intake air temperature	310K
Coolant temperature	15-90° C
Con rod length	139.5mm
RPM	2000
Inlet valve opening (IVO)	356 CAD aTDC
Intake valve closing (IVC)	578 CAD aTDC
Exhaust valve opening (EVO)	145 CAD aTDC
Exhaust valve closing (EVC)	357 CAD aTDC

**Table 2.1:** Engine specifications

### 2.1.1 Boundary conditions

Since some parts of the cylinder are not stationary, while some do not come in contact with fuel and have different physical properties (temperature, etc) due to being in contact with cooling liquid etc, the cylinder geometry is divided into 20 individual boundaries in *boundary* option of the geometry menu in the software. This gave the freedom to define the properties of each boundary individually, and further define their

behaviour upon contact with fluids appropriately, which was accomplished using *boundary conditions* menu under case setup.

Compared to others, some of the regions such as inlet valves, exhaust valves are divided into a number of smaller boundaries. This is due to the translating motion of some of its parts and to achieve fine meshing (achieved by using fixed embedding) as the air passes through/around them.

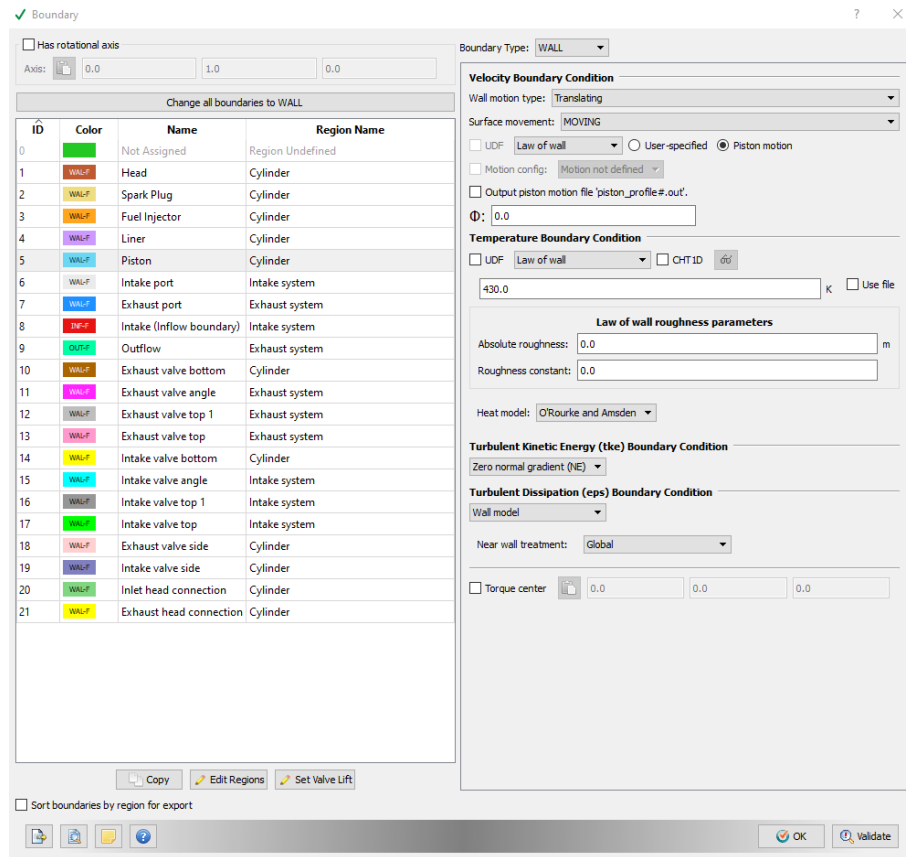


Figure 2.3: Boundary conditions [3]

The boundary conditions can be used to predominantly define,

- Boundary temperature.
  - Wall motion type.
  - Surface movement.
  - Turbulent kinetic energy.
  - Profile, etc.
- **Boundary temperature:** The individual boundaries defined in the cylinder have temperatures ranging from 310-600 K. Although different boundaries have different temperatures, but once defined it is constant throughout that boundary i.e. in reality the temperature in that boundary region (for eg: Piston) may vary over the surface, the software assumes it to be a constant and thus bringing some discrepancy to the results in the simulation compared to that of experimental setup with similar operating conditions.
  - **Wall motion type:** There are several types of motion like translating, rotating, arbitrary etc. Even though the simulation doesn't start at *0 seconds* or *0*

*CAD*, the position of the constant speed translating boundaries are adjusted as though the simulation started at 0 *CAD*, and moved to that position of starting *CAD*.

- **Profile:** Position of the translating boundaries in the cylinder geometry such as piston, inlet, exhaust valves need to be defined with respect to the global coordinates for each *CAD*. These profiles were obtained from the experimental setup and added into the case setup in the simulation.

### 2.1.2 Spray modeling

The liquid fuel and its properties in the simulation are defined in spray modeling menu, under physical models in the case setup.

Some of the important parameters defined in *spray modeling* are,

<b>Parcel species</b>	iso-octane, n-hexane, n-decane
<b>Mass fraction in 3 component fuel</b>	0.45, 0.35, 0.2
<b>Start of injection</b>	-310 <i>CAD</i>
<b>Fuel temperature</b>	335K
<b>Injection duration</b>	1.65ms or 19.8 <i>CAD</i>
<b>Total injected mass</b>	29.28 mg
<b>Number of nozzles</b>	6
<b>Nozzle diameter</b>	1.77 mm

**Table 2.2:** Spray modeling parameters

- **Parcel species and mass fraction:** A parcel is what the software solves instead of a drop. A parcel usually undergoes various processes such as breakup, coalescence, evaporation, etc. In a multi-component fuel mass fraction of each parcel is defined to represent the liquid fuel injected.
- **Injection duration:** The value for injection duration (1.65ms) obtained from experimental setup was converted to *CAD* as follows,

$$\omega_{(\text{rad.s}^{-1})} = \frac{2\pi}{60} \cdot N_{(\text{rpm})}$$

In this case  $\text{RPM} = 2000$ ,

$$\omega = 209.44_{(\text{rad.s}^{-1})} \quad \text{or} \quad 12000_{(\text{deg.s}^{-1})}$$

$$\text{Injection duration}_{(\text{CAD})} = 12000 * 0.00165$$

$$\Rightarrow 19.8$$



- **Total injected mass:** The mass of fuel injected in each cycle was calculated using the RPM and mass flow rate as follows,

$$Mass\ flow\ rate = 0.488_{(g.s^{-1})}$$

$$Mass\ per\ cycle = \frac{Mass\ flow\ rate * 720 * 60}{2000 * 60} \quad (kg.cycle^{-1})$$

- **Nozzle diameter:** To achieve the same injection pressure as the experimental setup ( $\approx 200$  bar), the nozzle diameter was decreased from 2mm to 1.77mm

### 2.1.3 Drop evaporation

Drop evaporation, which is an immense part of the mixing process is governed by Frossling correlation in the CONVERGE CFD modeling. More than 50% of injected fuel comes in contact with the high temperature (400-450K) surfaces of piston and liner. Although some of it is rebounded or splashed upon contact, the amount remaining on those surfaces is still significant and plays an important role in the mixture concentration.

The Frossling correlation is given by,

$$\frac{dr_0}{dt} = -\frac{\alpha_{spray} \rho_g D}{2\rho_l r_0} B_d Sh_d \quad [2]$$

where,

- $\alpha_{spray}$  is the vapor mass fraction at the drop surface
- $D$  is mass diffusivity of liquid vapour in air.

$$B_d = \frac{Y_1^* - Y_1}{1 - Y_1^*} \quad [2]$$

- $Y_1^*$  is vapour mass fraction at the drop surface
- $Y_1$  is vapour mass fraction
- $Sh_d$  is Sherwood number given by,

$$Sh_d = \left(2.0 + 0.6Re_d^{1/2} Sc^{1/3}\right) \frac{\ln(1 + B_d)}{B_d} \quad [2]$$

### 2.1.4 Drop wall interaction

#### 2.1.4.1 Wall film model

For drop wall interaction the CONVERGE software uses particle based wall film for modeling. It usually uses a hybrid technique by assuming particle based quantities for few calculations and film based quantities for others [2].

$$h_\alpha = \frac{\sum_p V_p}{|A_{\alpha,i}|} \quad [2]$$

where,

- $h_a$  is the film thickness on wall face a.
- $V_p$  is the parcel volume of the parcel p.
- $A_{a,i}$  is the area projection vector for face a.

#### 2.1.4.2 Drop/Film rebound

When the weber number of the droplets is lower than  $w_{rebound}$  specified in spray modeling, the drops are assumed to rebound. The weber number defined in spray modeling is given by, [2]

$$We_i = \frac{\rho_l V_n^2 d}{\sigma} \quad [2]$$

where,

- $\rho$  is the density of the liquid.
- $V_n$  is the component of drop velocity normal to the surface.
- $d$  is the drop diameter.
- $\sigma$  is the surface tension.

#### 2.1.4.3 Drop/film splashing

Drop/film splashing is defined by using Kuhnke model in simulations.

Splashing of a parcel in Kuhnke model is performed by equating the K number of the parcel, to the splash critical K number[2].

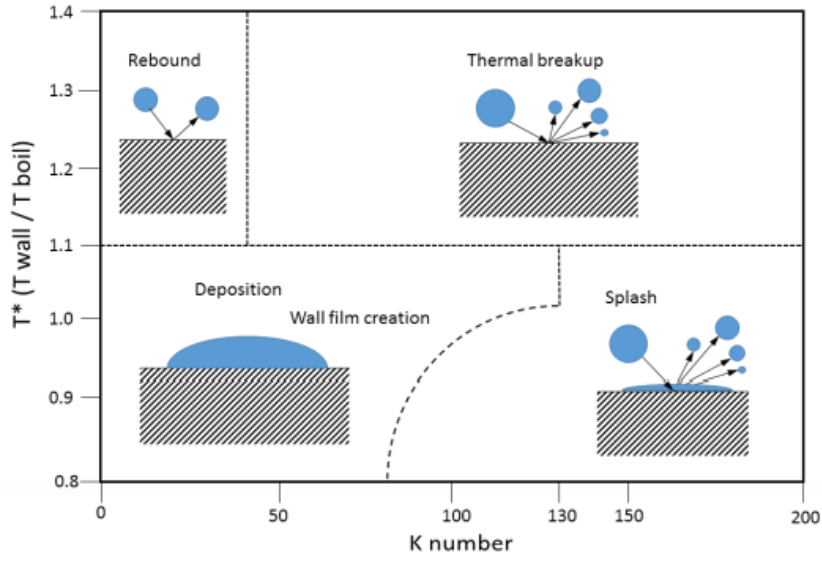


**Figure 2.4:** Possible parcel wall interaction outcomes in Kuhnke model [2].

The K number of liquid parcel is given by,

$$K = \frac{(\rho d)^{3/4} U^{5/4}}{\sigma^{1/2} \mu^{1/4}} \quad [2]$$

Which can also be written as,

$$K = We^{5/8} La^{1/8} \quad [2]$$

where,  $We$  is the weber number.  $La$  is the Laplace number given by,

$$La = \frac{\sigma \rho L}{\mu^2} \quad [2]$$

- $L$  is the diameter of the parcel.
- $\mu$  is the fluid viscosity.
- $\rho$  is the density.
- $\sigma$  is the surface tension.

### 2.1.5 Spray breakup

The CONVERGE software uses KH-RT (Kelvin-Helmholtz, Rayleigh-Taylor) model to solve the spray breakup.

### 2.1.5.1 Kelvin-Helmholtz model

The drop breakup size is determined by,

$$r_c = \frac{\sigma^2}{2\rho_g^2 U^3 v_g} \quad [2]$$

where,

- $r_c$  is breakup drop radius.
- $r_0$  is liquid jet radius.
- $\rho_g$  - density of inviscid gas.
- $U$  liquid jet radius.
- $\rho_l$  liquid density.
- $\mu_l$  viscosity of the liquid.

### 2.1.5.2 Rayleigh-Taylor model

Along with KH model the RT instability also causes spray breakup. The model(RT) ignores both liquid and gas viscosities, the unstable RT waves are caused by quick deceleration of drops from drag force and its given by the equation,

$$\omega_{RT} = \sqrt{k_{RT} \left( \frac{\rho_l - \rho_g}{\rho_l + \rho_g} \right) a - \frac{k_{RT}^3 \sigma}{\rho_l + \rho_g}} \quad [2]$$

- $\omega_{RT}$  - RT growth number.
- $\rho_l$  - liquid density.
- $\rho_g$  - Density of inviscid gas.
- $K_{RT}$  - wave number

In the converge CFD software both models can be ran concurrently,

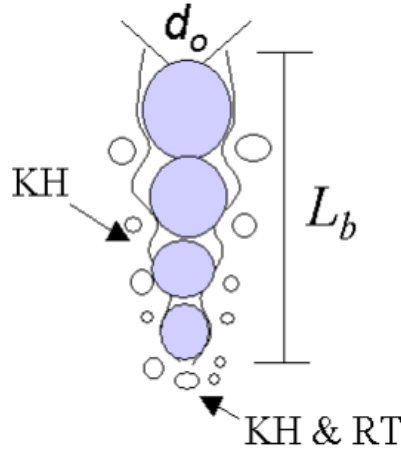


**Figure 2.5:** Schematic of the KH-RT spray breakup model [2]

$$L_b = C_{bl} \sqrt{\frac{\rho_l}{\rho_g}} d_o \quad [2]$$

As shown in figure [2.5] the model initially checks if RT model is responsible for breaking up the droplets, if not the KH model is employed.

In general the KH model is responsible for droplet breakup within the characteristic breakup distance  $L_b$ , beyond that distance both KH and RT models are activated [2]

### 2.1.6 Regions and Initialization

Converge CFD defines collection of boundaries as a region. Each region can be given a set of parameters apart from the parameter setup individual boundaries already have.

The geometry of the engine used is divided into three following regions:

- Cylinder
- Intake System
- Exhaust System

Each of the above regions are initialised with a set of parameters, among which Temperature, Pressure and the mass fraction of gaseous elements that are present inside the region prior to starting the simulation were primarily focused upon.

The parameter setup with which simulations were run is shown in the Table [2.3],

Region	Cylinder	Intake System	Exhaust System
Temperature(K)	400	310	500
Pressure(Pa)	101325	101325	101325
Residual Gases	N2 O2 CO2 H2O	N2 O2	N2 O2 CO2 H2O

**Table 2.3:** Regions and initialisation parameter setup

### 2.1.7 Events

Events include instances such as controlling the motion of fluid between two boundaries. The opening and closing of the inlet valves and outlet valves is to be included in this section.

"CONVERGE has an option called 'Automatic Valve events' where it creates OPEN and CLOSE events based on specific valve lift profiles"[2] The valve lift profile which determines the movement of inlet and outlet valves with respect to CAD are uploaded.

The geometry's initial position prior to starting the simulation is important, which includes the exact positions of both inlet and outlet valves which needs to be in a closed state in this case. But, if the valve's upper surface comes in contact with the cylinder head which physically happens in real life, it triggers the intersecting triangles error. Hence in this case, there must be a minimum gap between the two boundaries involved in the event, which needs to be specified.

When the minimum gap is reached, Converge automatically creates a set of temporary triangles connecting the edges of both the boundaries involved, thus sealing the area which blocks the flow of fluid. And during the event of opening the valves, the triangles sealing the gap disappears once the valve moves beyond the specified minimum value, allowing the flow of fluid.

### 2.1.8 Grid control

A base grid size specifies the size of the three dimensional blocks that are defined as empirical elements of the geometry. The grid size has more to do with the simulation run-time and the accuracy of the results. Smaller grid size provides a more accurate result but increases the simulation run-time and vice versa.

There are certain options in Converge to reduce the simulation run-time by controlling the grid size by region or by the timing of events happening.

The following were used in the simulation:

### 2.1.8.1 Fixed Embedding

At the locations where it is critical to get accurate results, a finer resolution of grids is applied to the geometry using fixed embedding. While using fixed embedding an embed scale(positive integer) is defined to instruct the software regarding the refinement of grid at the specified location [2].

$$embed = \frac{basegrid}{2^{(embed\ scale)}} \quad [2]$$

A huge gain in saving the simulation run-time can be done by specifying the specific time period for which the fixed embedding must exist, which essentially refines the grids into finer elements only during a particular event at that specific region which is otherwise at a base grid size. This helps in extracting the accurate results, cutting down a huge part of simulation run-time. The region of a fixed embedding could be assigned to any space in the domain, where the initial setup for each embedding needs to be manually assigned.

The regions and specifics of the fixed embedding assigned under the geometry using which simulations were run, is explained below:

- **Cylinder Region**

The cylinder region where the most of fluid interaction takes place is an important region to capture the dynamics of the fluid, which influences the results such as air-fuel ratio, spray, temperature and pressure variations, etc. So, an embed scale of 2 is allotted throughout the whole simulation for the cylinder region.

- **Intake and Exhaust valve gaps**

The gaps between the intake/exhaust valves and the cylinder head through which the movement of gases (air and exhaust gases) occurs, is a crucial part which defines the mixing process that takes place after the intake valves open and escape of remnant gases after the combustion, since they affect the result of the simulation significantly.

Hence, the grids corresponding to this region was given an embed scale of 3 to refine the grids to a smaller size for the duration from the opening until closing of the respective valves. This helps in capturing an accurate movement of the gases along with reducing the simulation-run time by choosing to activate the embedding layer for a specific period of time, rather than to embed the area for the whole simulation run-time.

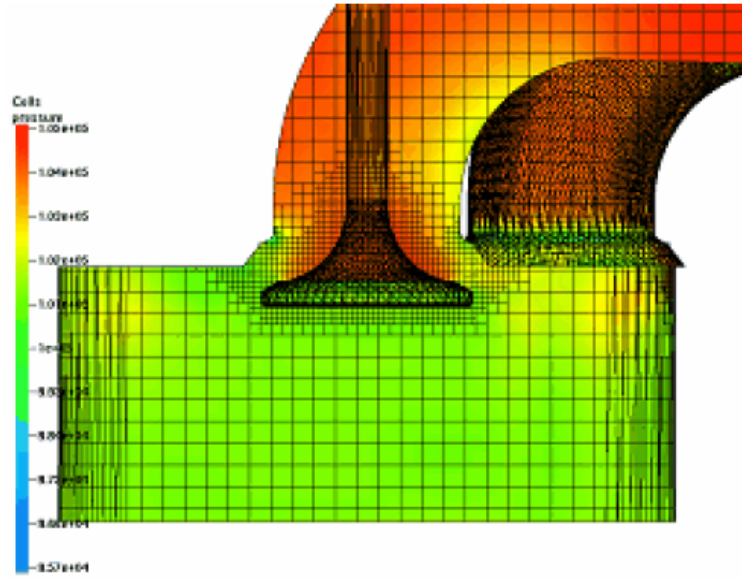


**Figure 2.6:** A visualisation of fixed embedding around the valve [2]

- **Spray area**

The fuel sprayed using an injector is designed to produce a spray cone. During the spray, thousands of fuel parcels (discrete packets of fuel) are ejected through the nozzles of the injector. There are a lot of possibilities for each parcel of fuel as to how and where they cease to exist depending on the environment it is interacting with. Most of the liquid parcels instantaneously vaporize into gaseous form of the fuel, due to the existing high temperature and pressure inside the cylinder, some end up on the piston and cylinder walls (liner) as liquid droplets. Thus it is crucial to capture dynamics of the liquid fuel spray. Hence, an embed layer in the shape of the cone adequate to capture the fuel spray is introduced for the duration of injection.

### 2.1.8.2 Adaptive Mesh Refinement (AMR)

AMR is used to define grid at the regions with unsteady flows such as temperature or velocity, automatically. This is helpful as it refines grid at the regions which are of interest and at the same time, it does not slow down the simulation [2].

As mentioned above, a fixed embedding of scale 2 was applied covering the cylinder region. But with the dynamics of fluid flow coming into the picture, it is critical to capture the finer details of changes in temperature, pressure and velocity of the flow of vaporized fuel-air mixture, which would require a more finer grid size than procured by the embed scale '2'.

Thus intake system and cylinder regions with an embed scale of '3' were selected, since this work concentrates on the pre-combustion events, AMR automatically refines the grids identifying quick changes in the required parameters such as temperature, velocity of fluid, etc, for the specific period of time saving a huge amount of



simulation run-time and giving detailed output of the required parameter particularly during the fuel spray and inlet of air into the cylinder.

## 2.2 Operating parameters

The initial case setup for the Volvo single cylinder medium tumble 4 valve GDI engine, which will be used as a reference to compare further simulations in the report was conducted with the following operating parameters,

Boundary	Temperature [K]
Piston	430
Liner	400
Inflow	310
Outflow	600
Cylinder head	400
Intake valve	380
Exhaust valve	380

**Table 2.4:** Boundary temperatures

These parameters were obtained from the experimental data, as they showed better results with good injection timing.

Except for that of piston, the boundary temperatures of all the individual boundaries remain unchanged i.e. in simulations the boundary temperature of the piston is varied to investigate its effect on mixing process.

Injection temp	335 K
SOI	-310 CAD
Simulation start	-380 CAD
Simulation end	-20 CAD

**Table 2.5:** Simulation parameters

The simulation was conducted from the start of intake stroke till the end of compression stroke (just before ignition timing), as the focus of the thesis is to study mixing processes and liquid film inside the cylinder.

The simulation time parameters i.e. start/end time will remain unchanged over entire simulations with different operating points.

### 2.3 Multi component fuel

Gasoline has boiling range of 307-470K, whereas iso-octane has a boiling temperature of 372K, below which it would not evaporate unlike gasoline. And similarly when the temperature inside the cylinder goes beyond 373K all the fuel (iso-octane) is vaporised. Thus, to accommodate the vaporisation profile [2.7] of gasoline, 2 fuels (n-hexane, n-decane) with lower and higher boiling points respectively, than that of iso-octane were selected for multi-component fuel (MCF) blend.

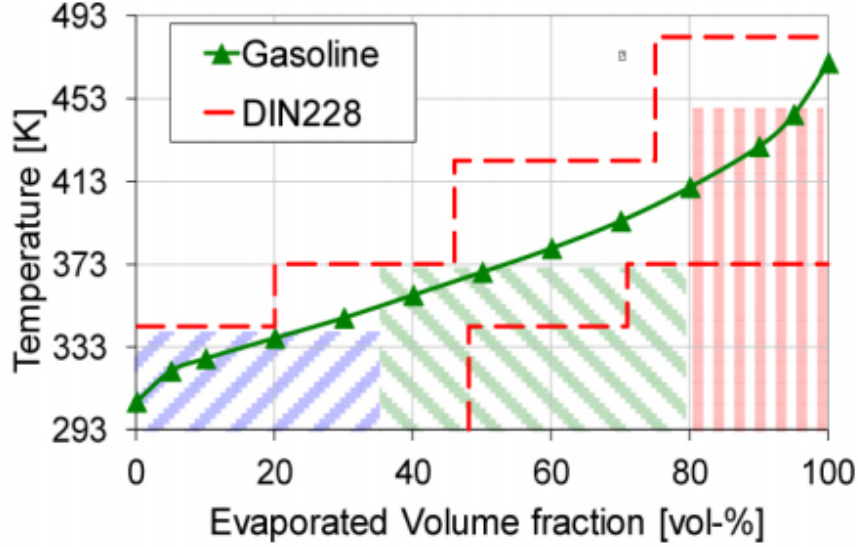


Figure 2.7: Vaporisation profile [5]

Fuel	Density [kg/m <sup>3</sup> ]	Saturation temp[K]	LHV[MJ/kg]
Gasoline	740	304-470	43.40
iso-octane (IC <sub>8</sub> H <sub>18</sub> )	699	372	44.65
n-hexane (nC <sub>6</sub> H <sub>14</sub> )	661	342	45.09
n-decane (nC <sub>10</sub> H <sub>22</sub> )	722	447	44.59

Table 2.6: Fuel properties of Gasoline and multi-component fuel

This blend was selected based on their Lower heating value (**LHV**) and density compatibility with the gasoline.

$$LHV_{(\text{gasoline})} = \sum LHV_i * m_i$$

Where,

- $LHV_i$  - LHV of individual surrogate fuel.
- $m_i$  - Mass fraction.

$$\Rightarrow (0.45 * 44.65) + (0.35 * 45.09) + (0.2 * 44.59)$$

$$LHV_{(\text{blend})} = 44.72$$

Which is close to that of gasoline (43.40 MJ/kg).

Since the focus of the thesis is mixing, density also plays an important role in selection and composition of the blend. As the density of the components in the blend are close to that of gasoline [2.6], this blend was selected for simulations.



# 3

## Results and discussion

For convenience the results section is divided into,

1. **Reverse flow into intake manifold.**
2. **Single component fuel.**
3. **Multi component fuel.**

In the latter two sections, results of following parameters are discussed,

- **Baseline simulation:** A simulation was conducted with the piston temperature of 430K and fuel temperature 335K as a baseline for comparing further simulations.
- **Piston film mass:** Amount of fuel reaching piston and rate of vaporisation.
- **Mixing process:** The equivalence ratio which is calculated using the formula,

$$\phi = \frac{FAR}{FAR_{(Stoic)}}$$

which is a ratio of actual fuel to air ratio(FAR), to stoichiometric fuel to air ratio.

- **Pressure and temperature:** The temperature and pressure profiles and trend inside the cylinder, over the course of simulation.

### 3.1 Reverse flow into intake manifold

As the intake valves close after the start of compression stroke, a reverse flow of the fuel-air mixture was encountered in all the cases.

RAM effect is a phenomenon which occurs when the piston is slowing down at BDC, the inertia of air inside the intake manifold increases the pressure, and continues charging until the inlet valves are closed when the engine speed is high. This effect is taken into advantage by closing the intake valves 40-60° after BDC[4].

The engine used in this thesis has a valve lift profile designed to take advantage of RAM effect at high speeds. As the operating speed is 2000RPM(lower engine speed) in this study, the reverse flow of fuel is more pronounced due to the low speed, pressure difference, when the piston starts moving towards TDC.

#### 3.1.1 Reverse flow with single component fuel

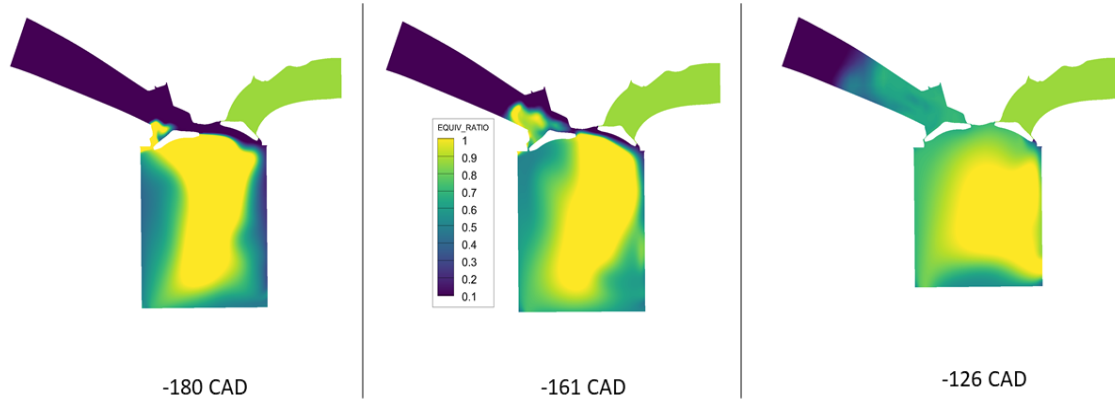


**Figure 3.1:** Reverse flow of iso-octane

Figure [3.1] shows equivalence ratio distribution inside the cylinder, it is observed that the reverse flow of fuel starts from  $\approx -180$  CAD, when the piston is beginning to move to TDC.

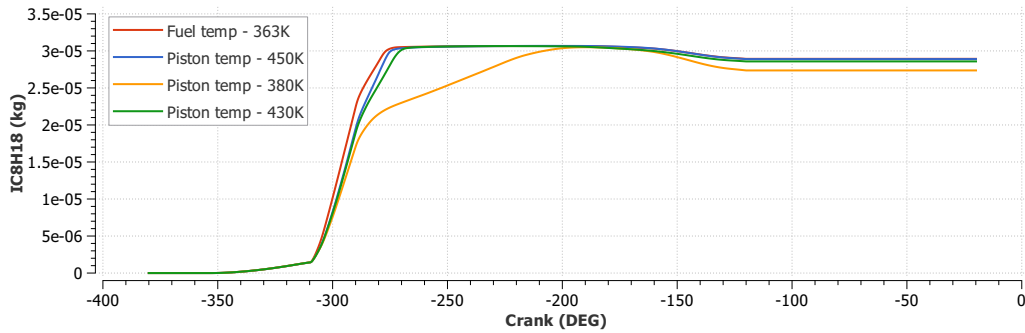


**Figure 3.2:** Fuel back flow with iso-octane

In the plot [3.2] it can be observed that the fuel starts escaping into intake manifold around  $-180$  CAD, due to the pressure difference as the piston starts moving from BDC to TDC. This trend of reverse flow into the intake manifold continues as long as the inlet ports are open i.e. until the CAD  $-126$ . After which the amount of fuel in the cylinder stays constant.

For the case when the piston temperature is 380K the evaporation takes longer, thus a slow trend in the increase of fuel mass inside the cylinder is observed [3.2].

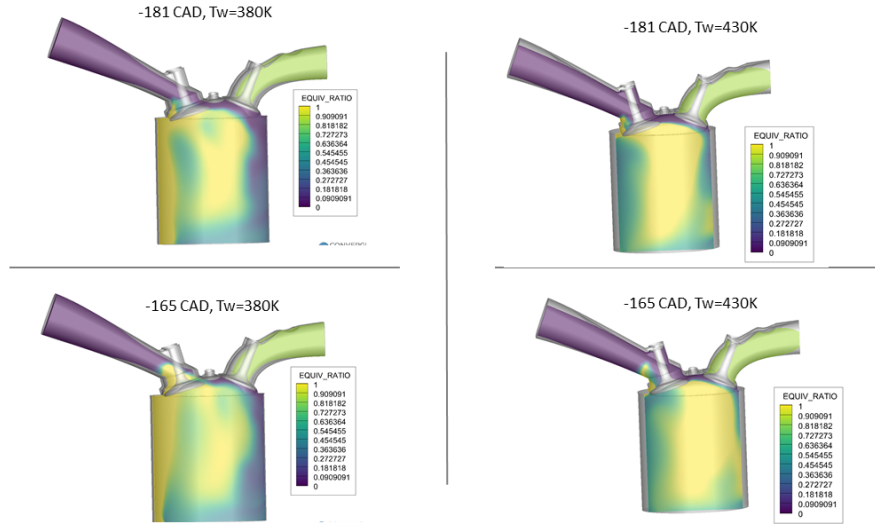


**Figure 3.3:** Fuel back flow with iso-octane [Tw 380 vs 430K]

It was noted that the highest fuel back flow with single component fuel takes place at the lowest piston temperature (380K)[3.2], this is due to the concentration of rich fuel-air mixture in the vicinity of the inlet ports, compared to the case when the piston temperature is 430K as shown in figure [3.3]

### 3.1.2 Reverse flow with multi-component fuel

Similar to the Single component fuel, simulations with Multi-component fuel also exhibited reverse flow into the intake manifold when the piston started moving to TDC from BDC.

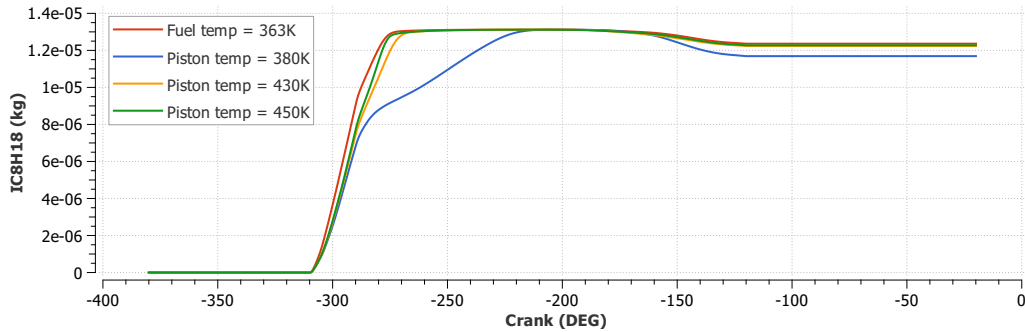


**Figure 3.4:** Fuel back flow of iso-octane in MCF

As seen from the plot [3.4], which shows the iso-octane mass in the cylinder over the simulation period, the reverse flow trend of fuel follows that of single component

fuel as shown in [3.2].

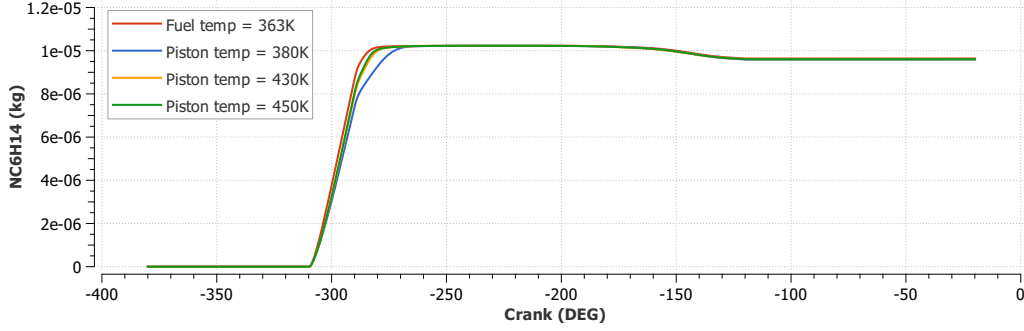


**Figure 3.5:** Fuel back flow of n-hexane in MCF

n-hexane with a lower boiling temperature of 342K evaporates quicker compared to iso-octane, therefore the slow evaporation curve (when  $T_w=380K$ ) is not encountered. Similar to iso-octane the reverse backflow starts when the piston starts moving back to TDC from BDC ( $\approx -180$  CAD), and the escape continues until the intake valves are closed at -126CAD.

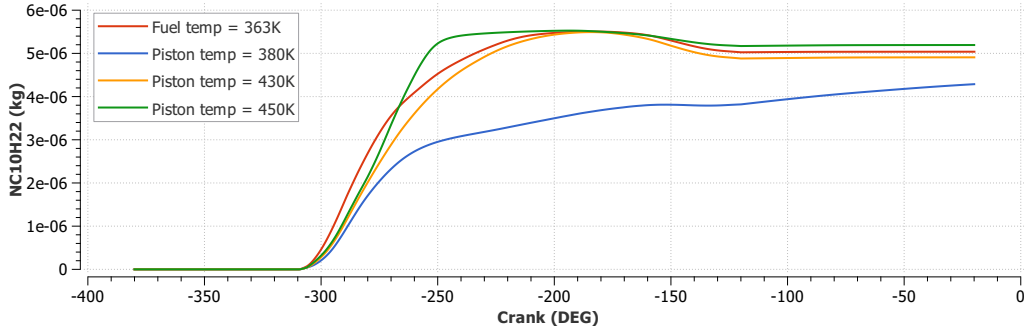


**Figure 3.6:** Fuel back flow of n-decane in MCF

As seen in the plot [3.6] n-decane with higher boiling temperature evaporates slower than the other 2 components of the blend. For all the cases except when the piston temperature is 380K, the fuel evaporation tends to follow a trend similar to that of single component fuel.

When the piston temperature is 380K which is much lower than the boiling temperature of n-decane (447K), the curve is seen to gradually increase, in contrast to other cases which see a rapid rise in n-decane mass inside the cylinder, and the reverse flow is also encountered later (between -150 & -126 CAD), than the other cases.

Unlike the other 2 components of the blend which have completely evaporated, due to the increase in pressure and temperature, n-decane continues to evaporate after the intake valve closes, and it continues until the end of simulation.



The maximum fuel escaped in the simulations was  $\approx 5\%$ , all of which will re-enter as a pre-mixed, lean, homogeneous mixture when the inlet valves open in the next cycle. Therefore this phenomenon is assumed to have minimal impact in this cycle, and its effect is ignored as it is beyond the scope of study of the thesis.

## 3.2 Single component fuel

### 3.2.1 Baseline simulation

An initial simulation with operating parameters described in [2.4][2.5] was conducted as a baseline to compare the results from further simulations, which were performed with changes made in the operating parameters.

The results of the baseline simulation are collated with that of further simulations, to get a better understanding of the effects of changes made in operating parameters.

#### 3.2.1.1 Pressure

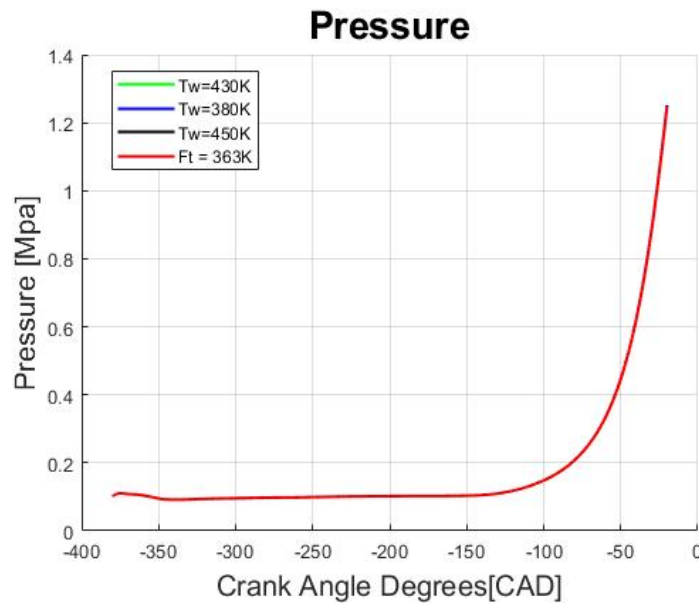


**Figure 3.7:** Pressure inside the cylinder

The pressure profile inside the cylinder during the simulation is shown in [3.7], it is identical for all the cases with different operating parameters (change in piston and fuel temperature).

The Pressure inside the cylinder is seen to increase when the piston starts from to TDC around -180CAD, at the end of compression stroke (-20 CAD) the peak pressure is **1.25 Mpa**.

The further simulations with single component fuel with varying operating parameters as mentioned above, showed the identical pressure profiles with no considerable deviation compared to the baseline simulation with pressure peaking around 1.25 MPa at -20 CAD.

### 3.2.1.2 Fuel film mass on piston

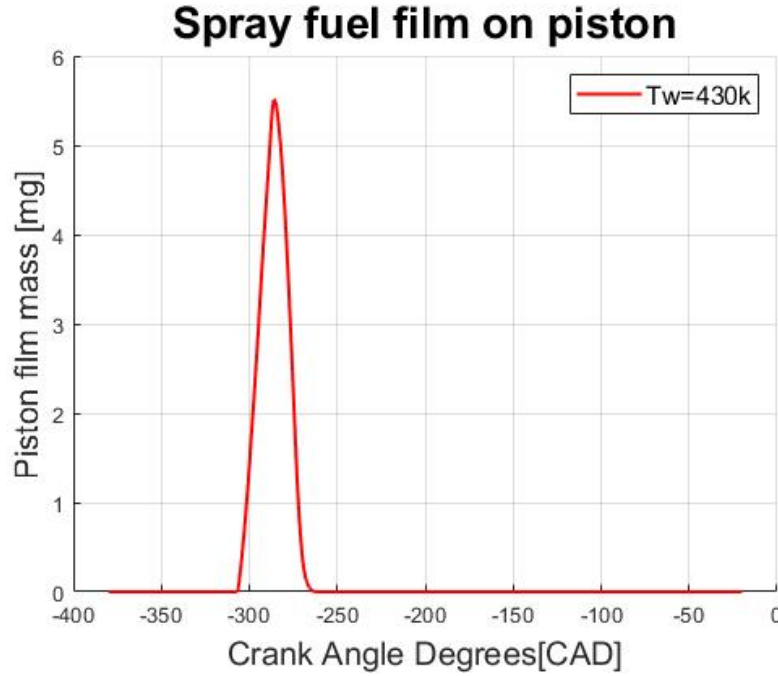


**Figure 3.8:** Fuel film mass on piston

The injection of fuel into the cylinder starts at -310 CAD, but the actual increase in the mass of the fuel on the piston is seen after few CAD i.e. at -306 CAD [3.8]. The amount of fuel on the piston returns to zero at -263CAD i.e. after 43CAD from the initial spike.

The peak fuel mass sitting on the piston is 5.5mg which is at the -285 CAD.

### 3.2.1.3 Mixing

To study the mixing process the equivalence ratio plot is obtained from Tecplot for CONVERGE, by inserting a slice in the Y axis of the cylinder and equivalence ratio distribution histogram is obtained from CONVERGE.

Figure [3.9] represents the equivalence ratio at -20 CAD (end of compression stroke). The image above in the figure visually represents the distribution of fuel-air mixture in the cylinder at a two-dimensional plane passing through the centre of the cylinder. The image below consisting the histogram shows the complete distribution of fuel-air mixture inside the cylinder.

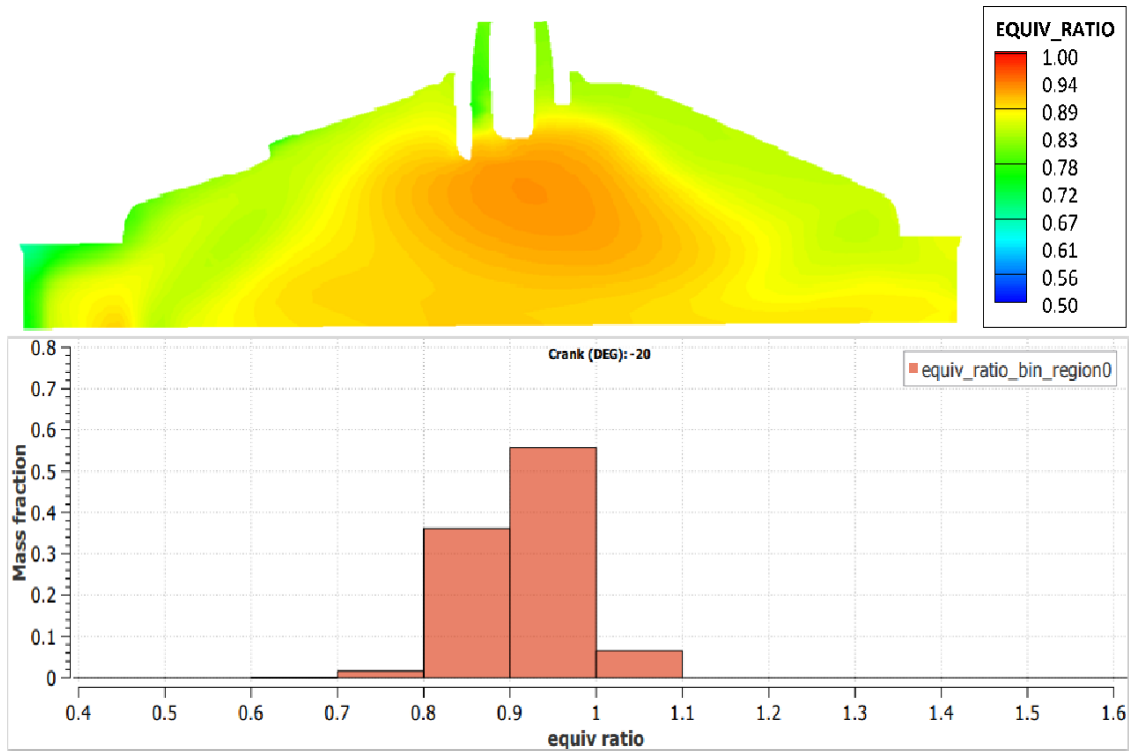


**Figure 3.9:** Equivalence ratio distribution with Piston temperature at 430K

The image shows the existence of fuel rich mixture of equivalence ratio around 0.95 (Orange region) in the central part of the cylinder and the charge gets leaner gradually moving away from the centre with equivalence ratio ranging from 0.89 (Yellow region) to 0.80 (Green region) as we move towards the cylinder wall.

As represented by the histogram, a total of 55% of mixture is at an equivalence ratio between 0.9 and 1.0, 37% between 0.8 and 0.9, 8% between 1.0 and 1.1 and the rest of the mixture being leaner with equivalence ratio below 0.8. A high percentage of mixture with an equivalence ratio in a single band shows us that the mixture present in the cylinder at the end of compression stroke with piston temperature at 430K is a fairly homogeneous mixture and indicates that a good mixing has taken place.

### 3.2.1.4 Temperature

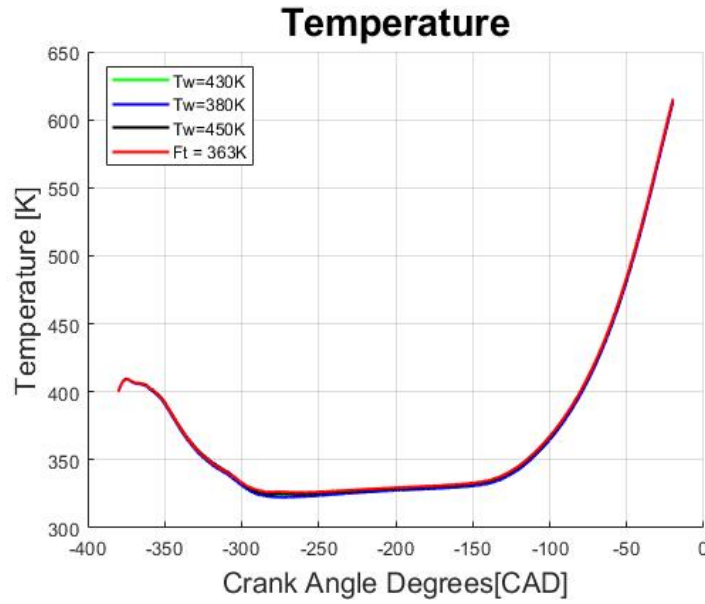


**Figure 3.10:** Temperature inside the cylinder for SCF

The temperature profile for all the cases is identical. As seen in the plot [3.10], at the start of intake stroke the temperature in the cylinder decreases for few CAD, as the incoming air is substantially cooler (310K) than the temperature of cylinder boundaries (400-430K). Hence the initial defined temperature of 400K inside the cylinder, goes down to 324K. The temperature inside the cylinder slightly increases until the start of compression stroke, after which we see a quick increase in its value, and the temperature at the end of compression stroke was **616K**.

#### 3.2.2 Fuel film mass on piston

In this section the piston fuel film mass i.e. the amount of fuel hitting the piston upon injection and its subsequent evaporation are discussed.

##### 3.2.2.1 Effects of varying surface piston temperature

To study the effects of piston fuel film mass on mixing at different surface temperatures, the piston temperature was changed from the initial value of 430K to 450K and 380K.

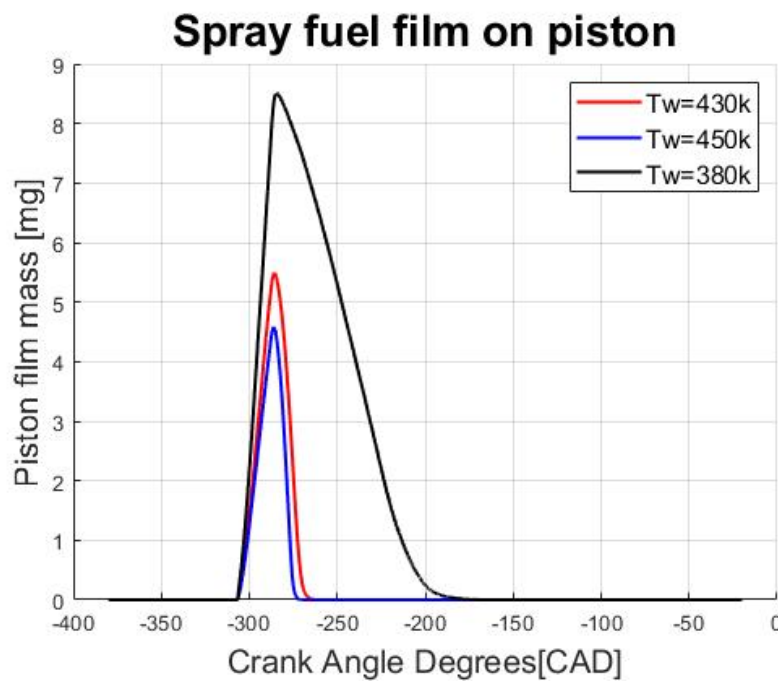


**Figure 3.11:** Fuel film mass on piston with varying piston temperatures

As shown in figure [3.11] amount of fuel, and the duration for film evaporation varies drastically for different piston temperature.

- At the piston temperature 450K, which is slightly higher than that of baseline temperature 430K and substantially higher than the boiling point of iso-octane (372K). The peak piston film mass seen at -285CAD decreases from 5.5 mg to 4.5 mg.
- At the same piston temperature the evaporation duration decreased from 43 CAD to 37 CAD.
- When the piston temperature was decreased to 380K, which is much lower than the earlier 2 cases. The peak piston mass increases from 5.5mg to 8.46 mg at -285CAD. This is due to slow evaporation rate i.e. the decrease in piston

temperature causes higher mass to accumulate before complete evaporation.

- At the same temperature [ $T_w=380\text{K}$ ] the complete evaporation duration substantially increases from 43CAD to 130CAD i.e. starting from initial spike at -306CAD, the fuel on the piston completely evaporates at -176CAD.

### 3.2.2.2 Effects of increasing fuel temperature

In the further cycles as the fuel passes through the tubes surrounded by components which are increasing in temperature, the fuel temperature also increases. Taking this into account, the fuel temperature was increased from the initial value of **335K to 363K**.

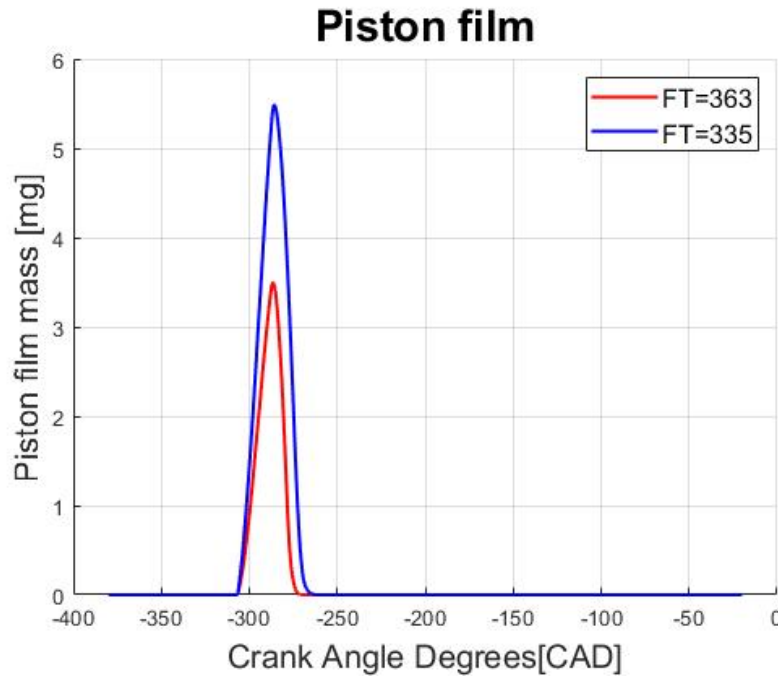


**Figure 3.12:** Fuel film mass on piston with Fuel temperature at 363K

As the boiling temperature of fuel is 372K, increasing the fuel temperature to 363K brought about quicker evaporation after coming in contact with the air inside the cylinder [400K] and the peak piston film mass reduced from 5.5mg to 3.5mg. The evaporation duration also decreased from 43 CAD to 35 CAD.

### 3.2.3 Mixing process

Mixing process is an essential step in the ICE operation. A good mixing not only gives better fuel efficiency but also reduces the particulate emissions. Thus achieving stoichiometric mixture is of high importance in this case.

#### 3.2.3.1 Piston temperature = 380K

Figure [3.13] represents the equivalence ratio at the end of compression stroke when the piston temperature is 380K.

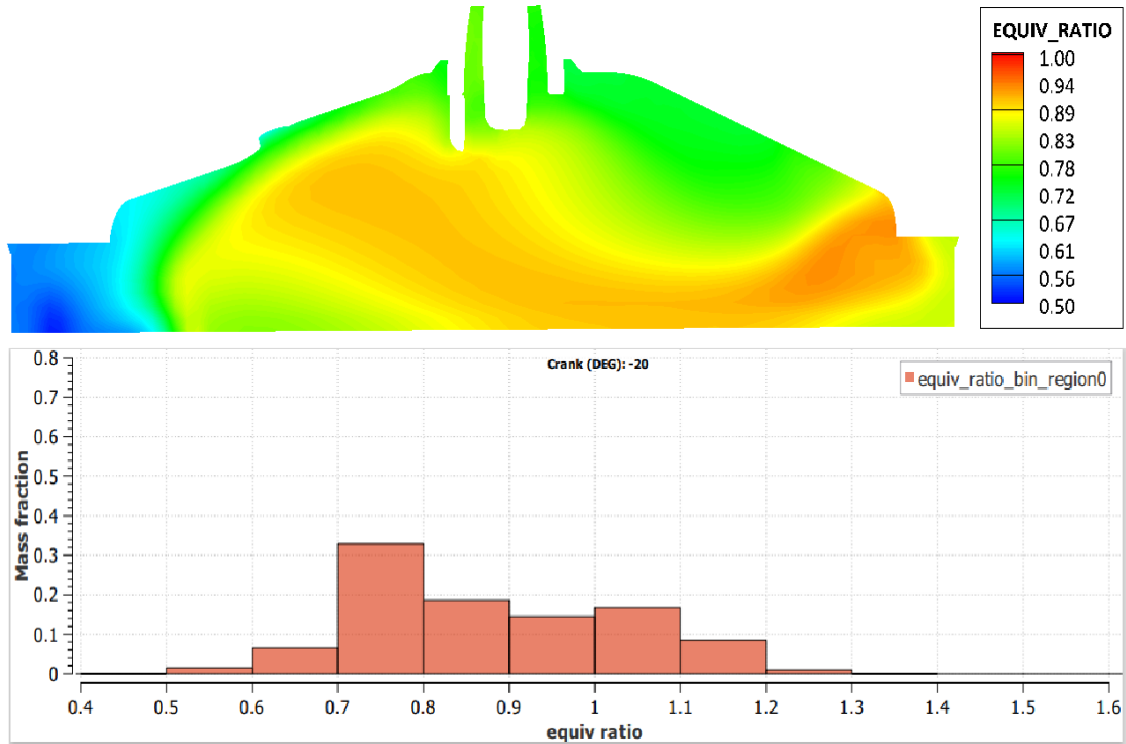


**Figure 3.13:** Equivalence ratio distribution with Piston temperature at 380K

The image shows the existence of fuel rich mixture of equivalence ratio around 1.0 (Red region) in the right-side of the cylinder which continues towards the centre with ER around 0.95 (Orange region) surrounded by ER around 0.87 (Yellow region). A leaner mixture pockets of ER at 0.78 (Green region) and 0.5 (Blue region) exist on the top right and left bottom of the cylinder, the clear distinction of different coloured bands represent the mixture to be stratified.

As represented by the histogram, a total of 34% of mixture is at an equivalence ratio between 0.7 and 0.8, 20% between 0.8 and 0.9, 16% between 0.9 and 1.0, 18% between 1.0 and 1.1, 9% between 1.1 and 1.2 and majority of the rest of the fuel being leaner with ER between 0.5 to 0.7. Considerable mixture of air-fuel distributed among the band varying from 0.6 and 1.2 confirms the presence of stratified mixture inside the whole cylinder with a majority of air-fuel mixture being leaner when the



piston temperature is at 380K compared to 430K as shown in figure [3.9], representing a poor mixing of the charge.

### 3.2.3.2 Piston temperature = 450K

Figure [3.14] represents the equivalence ratio at the end of compression stroke when the piston temperature is 450K.

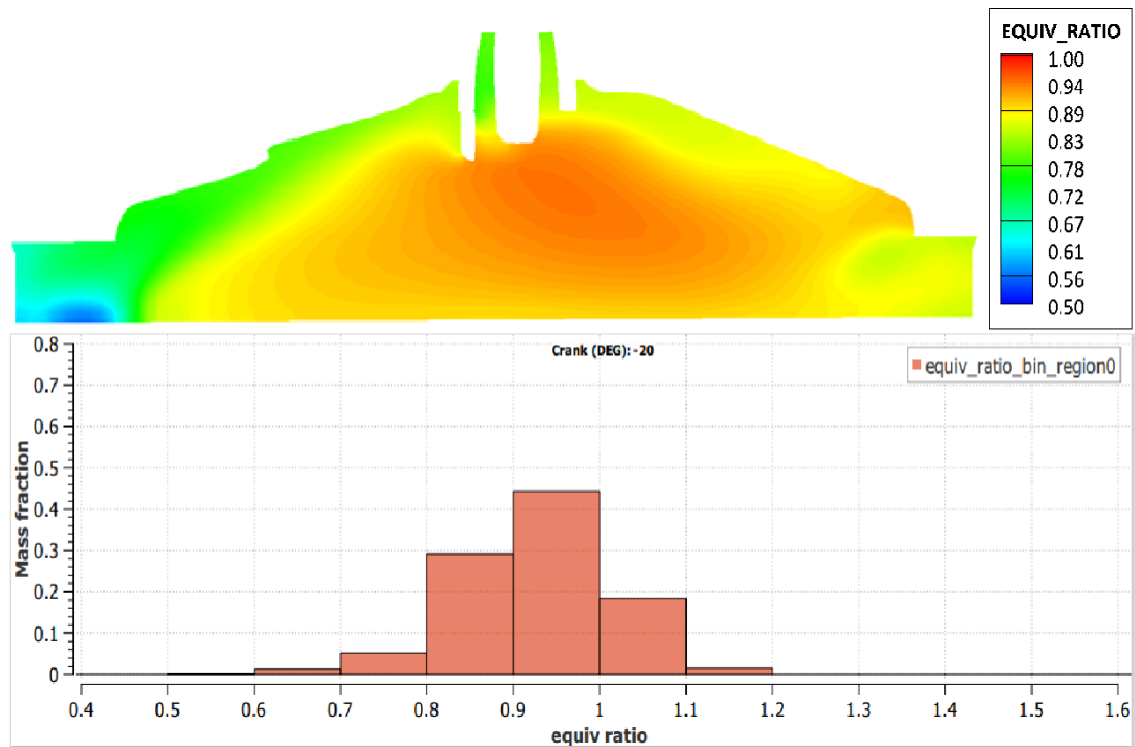


**Figure 3.14:** Equivalence ratio distribution with Piston temperature at 450K

The image shows the existence of fuel rich mixture of equivalence ratio around 0.95 (Orange region) in the central part of the cylinder surrounded by a region of mixture with ER around 0.89 (Yellow region). Leaner mixture pockets of ER 0.75 and 0.55 exist on the left side of the cylinder while the right side is comparatively has fuel rich mixture.

Histogram shows a total of 45% of mixture is at an equivalence ratio between 0.9 and 1.0, 30% between 0.8 and 0.9, 19% between 1.0 and 1.1, and majority of the rest of the fuel being leaner with ER between 0.5 to 0.8. A high percentage (94%) of fuel sits in the range between 0.8 and 1.1 representing a fairly homogeneous mixture with the presence of leaner charge pockets shows the mixing taken place to be better with piston temperature at 450K than 380K but poorer than 430K.

#### 3.2.3.3 Fuel temperature = 363K

Figure [3.15] represents the equivalence ratio at the end of compression stroke when the piston temperature is 450K.

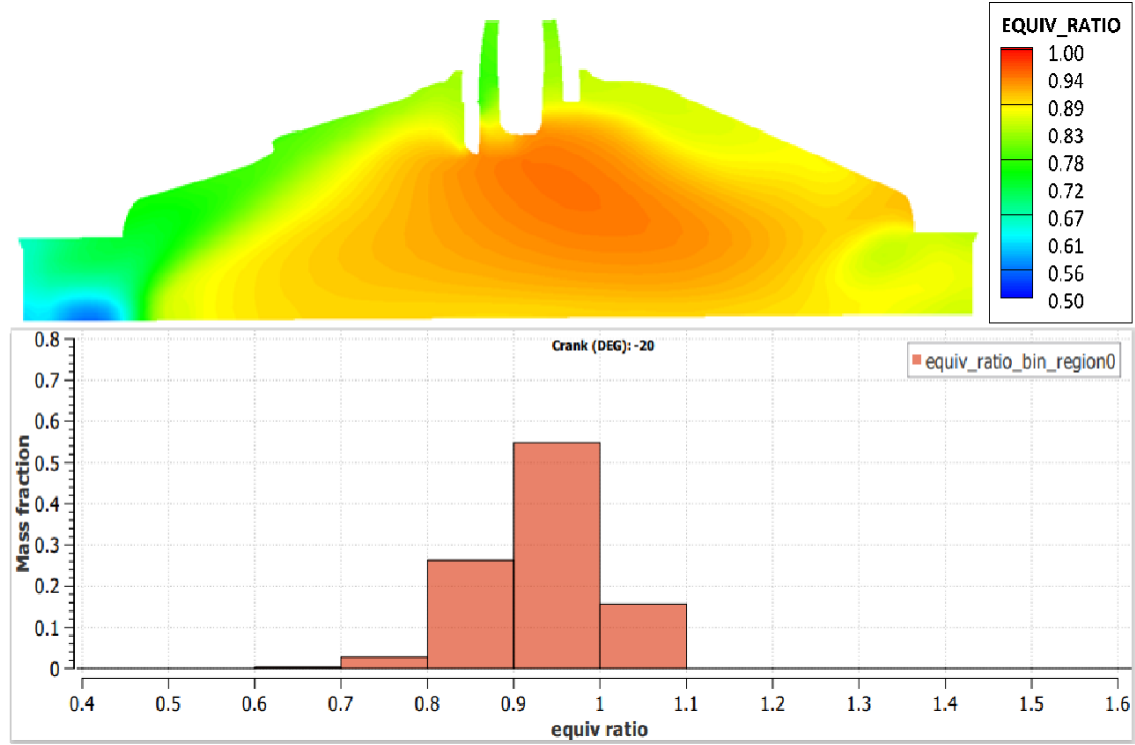


**Figure 3.15:** Equivalence ratio distribution with Fuel temperature at 363K

The image shows the existence of fuel rich mixture of equivalence ratio around 0.95 (Orange region) in the central part of the cylinder surrounded by a region of mixture with ER around 0.89 (Yellow region). Leaner mixture pockets of ER 0.75 and 0.55 exist on the left side of the cylinder while the right side is comparatively has fuel rich mixture.

Histogram shows a total of 55% of mixture is at an equivalence ratio between 0.9 and 1.0, 26% between 0.8 and 0.9, 16% between 1.0 and 1.1, and rest of the fuel being leaner with ER between 0.5 to 0.8. A high percentage (97%) of fuel ranging between 0.8 and 1.1 representing a fairly homogeneous mixture with the presence of leaner charge pockets shows the mixing taken place similar to that of fuel temperature at 335K.

### 3.3 Multi component fuel

Similar to single component fuel a baseline simulation was performed for MCF as well. This was used to compare and discuss the results of further simulations.

A total of four simulations were conducted among which one simulation with a parameter setup up as mentioned in [2.4][2.5] to be a baseline simulation. Further three simulations were conducted with varying individual operating parameters as mentioned below,

- Piston Temperature = 380 K
- Piston Temperature = 450 K
- Fuel Temperature = 363 K

The results from these simulations were compared with the baseline simulation, as well as to the Single Fuel Component simulation results of the corresponding parameter setup.

#### 3.3.1 Baseline simulation

An initial simulation with operating parameter setup as described in [2.4][2.5] was conducted as a baseline simulation whose results have been presented below.

##### 3.3.1.1 Pressure

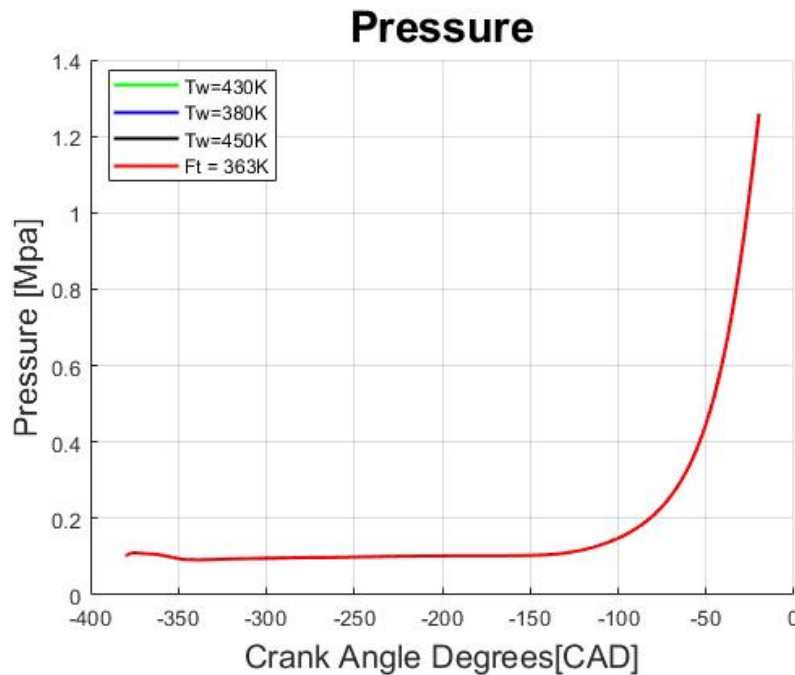
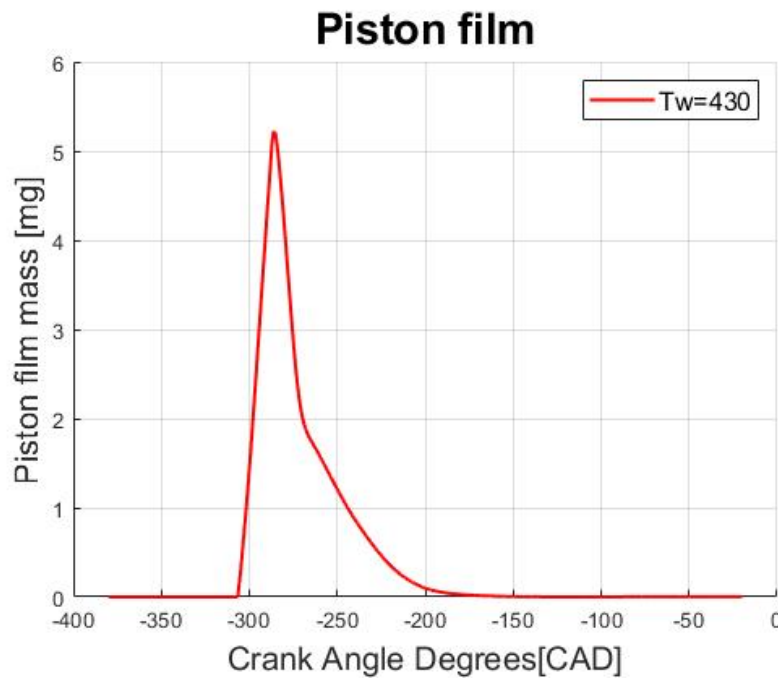


**Figure 3.16:** Pressure inside the cylinder for MCF

Figure [3.16] shows in-cylinder pressure profile over the simulation period, it is identical for all the cases with different operating parameters. As seen in the graph, the pressure starts increasing from -180 CAD from when the piston starts moving from BDC towards the TDC, the pressure peaks at the end of the compression stroke around 1.25 MPa at -20 CAD.

The further simulations using Multi component fuel with varying parameters as mentioned above, showed the identical pressure profile with no considerable deviation compared to the baseline simulation with pressure peaking around 1.25 MPa at -20 CAD.

#### 3.3.1.2 Fuel film mass on piston



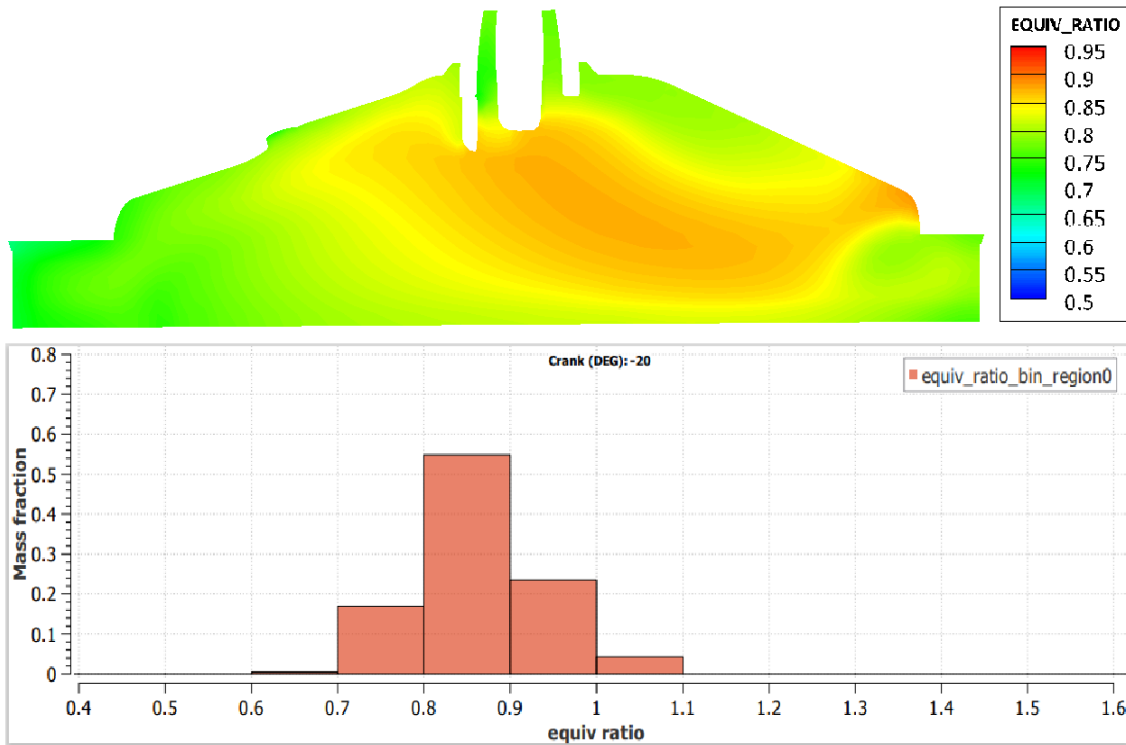
**Figure 3.17:** Fuel film mass on piston for MCF with Piston temperature at 430K

Figure [3.17] represents the fuel film mass deposited on the piston. The fuel is injected at -310 CAD, among which most of the fuel parcels get vaporized instantaneously due to the higher temperature that exists inside the cylinder. But, some amount of liquid parcels which is directly shot towards the piston which has not undergone vaporization settles on the piston. As it can be seen from the figure the fuel film mass on the piston increases quickly from the start of injection (-310 CAD) from 0 mg to 5.22 mg at -286 CAD which is just after the end of injection at -291 CAD. Further, a steep decline in the fuel film mass on piston is seen due to the heat being transferred from the piston surface which is at 430K through conduction as well as the surrounding high temperature that exists in the cylinder.

The fuel considered in this simulation include three components which are Iso-Octane, n-Hexane and n-Decane. The decline in fuel film mass on piston can be broken down into two stages with the differing slopes, one from CAD -286 to -269, and the second from CAD -269 to -146. The first stage has a steep decline compared to the second stage because it is observed that majority of the Iso-Octane and n-Hexane settled on the piston gets evaporated during this stage since they have a lower boiling point than that of n-Decane. The second stage sees a gradual decrease in the mount of fuel film on the piston surface which majorly consists of the component n-Decane that evaporates slower than Iso-Octane and n-hexane while the temperature and pressure in the cylinder gradually increases.

### 3.3.1.3 Mixing Process

Figure [3.18] represents the equivalence ratio at -20 CAD (End of compression stroke). The image above in the figure visually represents the distribution of fuel-air mixture in the cylinder at a two-dimensional plane passing through the centre of the cylinder. The image below consisting the histogram shows the complete distribution of fuel-air mixture inside the cylinder.



**Figure 3.18:** Equivalence ratio distribution with Piston temperature at 430K

The image shows the existence of fuel rich mixture of equivalence ratio around 0.9 (Orange region) in the central part of the cylinder and the charge gets leaner gradually moving away from the centre with equivalence ratio ranging from 0.85 (Yellow

region) to 0.70 (Green region) as we move towards the cylinder wall.

As represented by the histogram, a total of 54% of mixture is at an equivalence ratio between 0.8 and 0.9, 23% between 0.9 and 1.0, 17% between 0.7 and 0.8, 5% between 1.0 and 1.1 and the rest of the mixture being leaner between 0.6 and 0.7. A high percentage of mixture (about 95%) with equivalence ratio between 0.7 and 1.0 shows us that the mixture present in the cylinder at the end of compression stroke with piston temperature at 430K is a fairly homogeneous mixture and indicates that a good mixing has taken place.

#### 3.3.1.4 Temperature

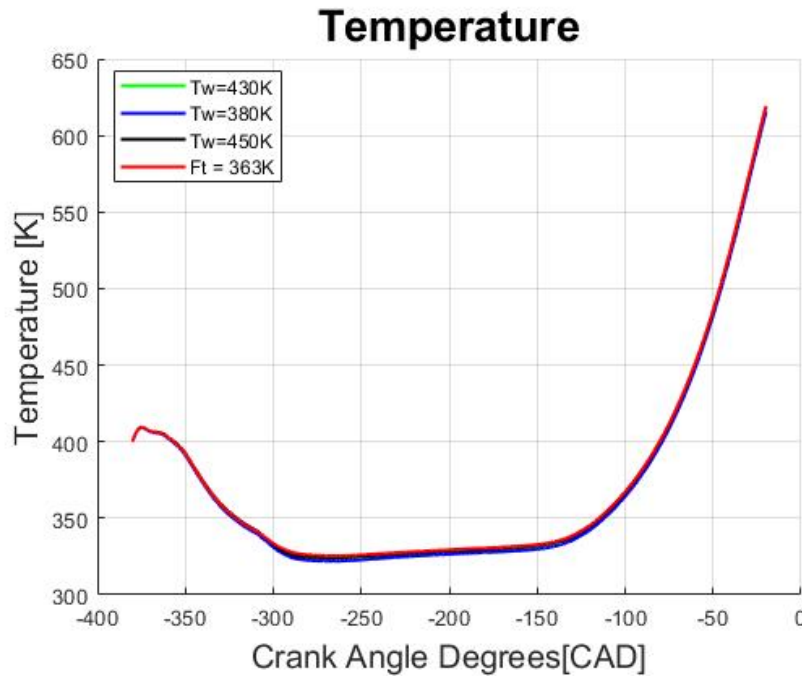


**Figure 3.19:** Temperature inside the cylinder for MCF

Figure [3.19] shows the Temperature profile inside the cylinder over the simulation period, it is identical for all the cases. As seen in the graph, the initial temperature inside the cylinder is 400K, then it gradually decreases due to the inlet valves opening at -360CAD allowing the relatively cold air (310 K) inside the cylinder dropping the in-cylinder temperature to around 325K. A steep increase in temperature is seen from -180 CAD when the piston starts moving from BDC towards TDC and it peaks at the end of compression stroke with temperature 617K.

Further simulations with varying parameters showed an identical temperature profile with no considerable deviations compared to the baseline simulation temperature profile.

### 3.3.2 Fuel film mass on piston

#### 3.3.2.1 Effects of varying surface piston temperature

Similar to single component fuel, to study its effect on mixing processes and film mass on piston, the initial piston temperature of 430K was changed to 380K and 450K for multi component fuel as well.

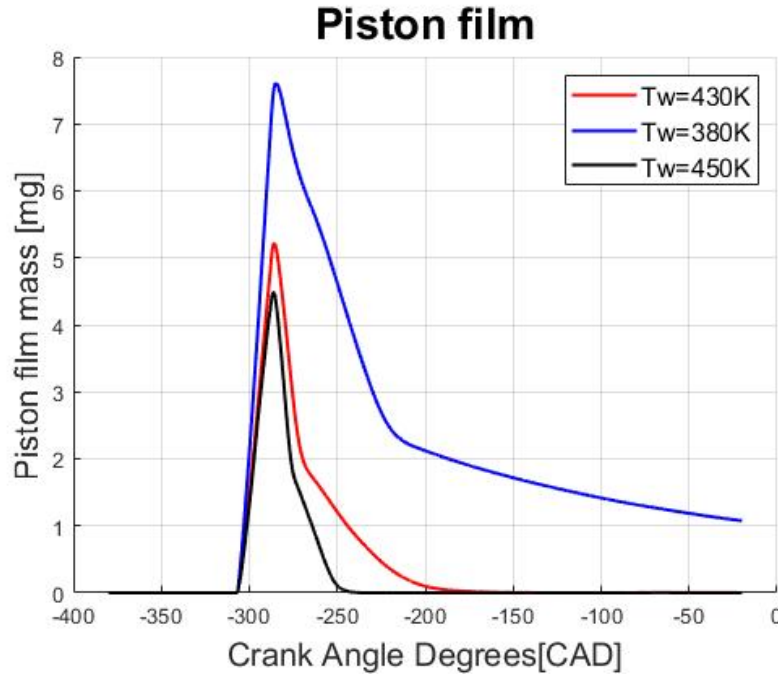


**Figure 3.20:** Fuel film mass on piston with varying piston temperatures for MCF

- For piston temperatures 380K and 450K the plot follows the same trend as that of the baseline simulation (430K).
- The fuel film deposition on piston for all the three simulations reach the peak around -286CAD. Showing a higher peak for 380K with 7.61mg and lower peak for 450K with 4.48mg.
- For the piston temperature at 450K, the first stage of drop in fuel film starts at -286CAD (peak) to -275CAD where majority of the Iso-Octane and n-Hexane is vaporized. The second stage immediately begins where the remaining fuel film containing n-Decane component starts evaporating. It takes a longer duration than the first stage, and gets completely evaporated at -236CAD.
- For the piston temperature at 380K, the peak which is slightly later at -284 CAD compared to the other two simulations, the first stage of evaporation lasts until -220 CAD and the second stage which begins at the same CAD does not see the complete evaporation of the fuel film which gradually decreases in amount until the end of simulation (end of compression stroke) with a fuel film mass of 1.07 mg still deposited on the piston surface. This residual fuel film mass on the piston will result in particulates upon combustion.

#### 3.3.2.2 Effects of increasing fuel temperature

Figure [3.21] represents the fuel film mass deposited on the piston surface for fuel temperature at 335K and 363K.

It can be observed that, the fuel film mass plot for fuel temperature 335K, follows the exact same trend when the piston temperature is 430K. When the fuel temperature is 363K we see a lower peak of 3.86mg, compared to 5.2 mg of 335K, at the same CAD of -286. The first stage of evaporation lasting from the peak to -273 CAD and the second stage ending at -182 CAD.

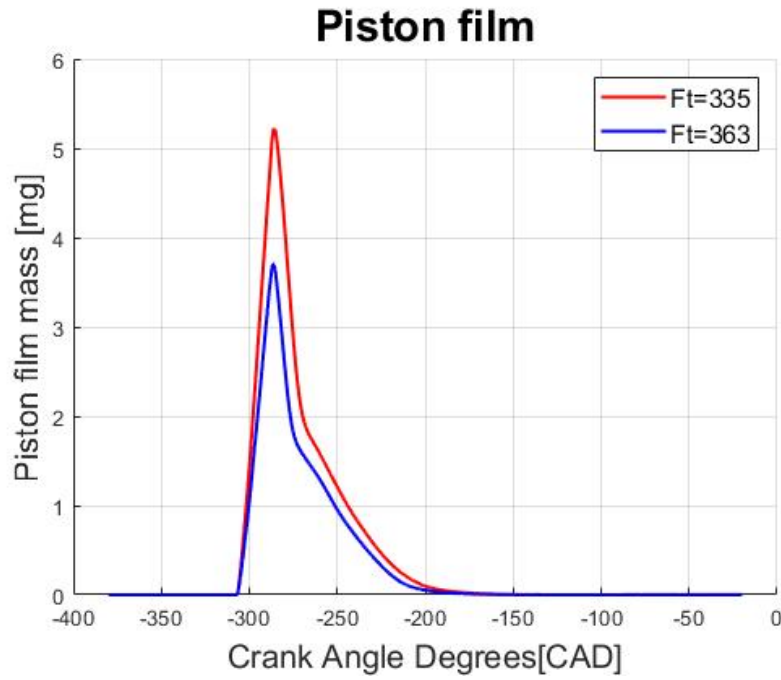


**Figure 3.21:** Fuel film mass on piston for MCF with Fuel temperature at 363K



### 3.3.3 Mixing process

#### 3.3.3.1 Piston temperature = 380K

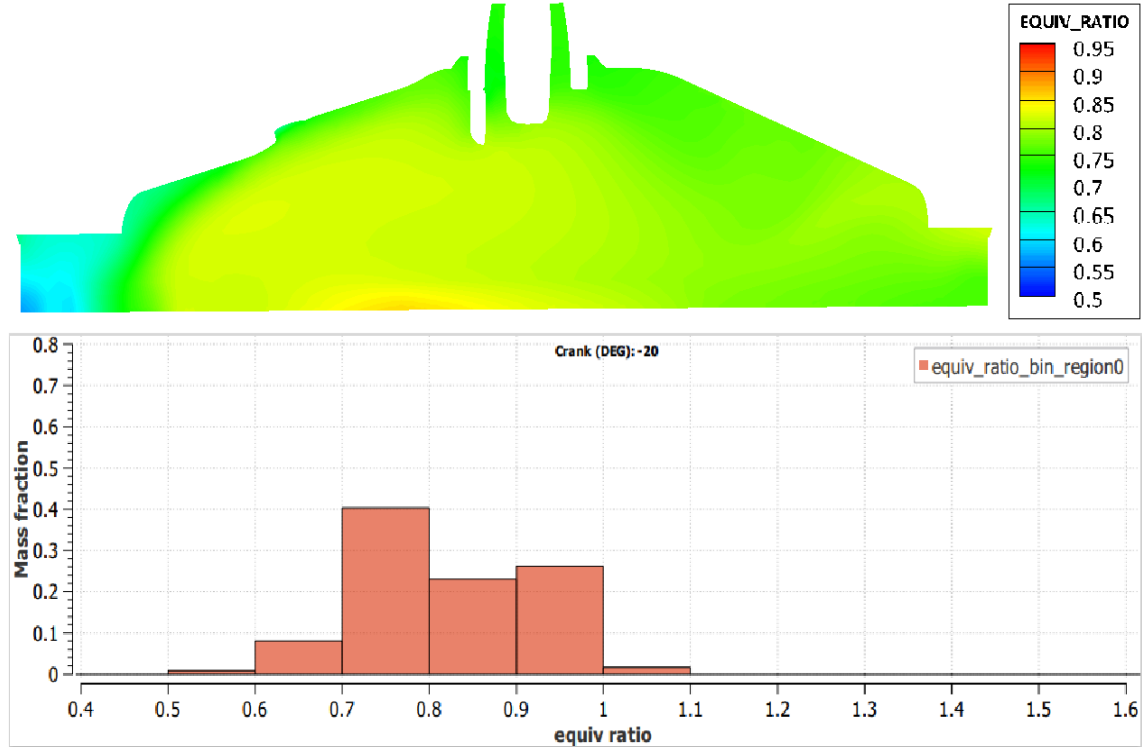


**Figure 3.22:** Equivalence ratio distribution for MCF with Piston temperature at 380K

In the Figure [3.22] the two-dimensional slice of cylinder shows the mixture to be leaner (mostly covered in green) and a blue pocket towards the left bottom, near the connection of piston and cylinder wall. This is confirmed by histogram with a majority 40% of mixture between E.R of 0.7 and 0.8, 22% between 0.8 and 0.9, 26% between 0.9 and 1.0. and the rest are rich and lean pockets near the piston.

Since the deposition of the fuel film on the piston surface is highest when the piston temperature is at 380K, and the fuel does not completely evaporate, it deprives the charge inside the cylinder of a considerable amount of fuel giving rise to a leaner mixture of charge as seen the figure.

#### 3.3.3.2 Piston temperature = 450K

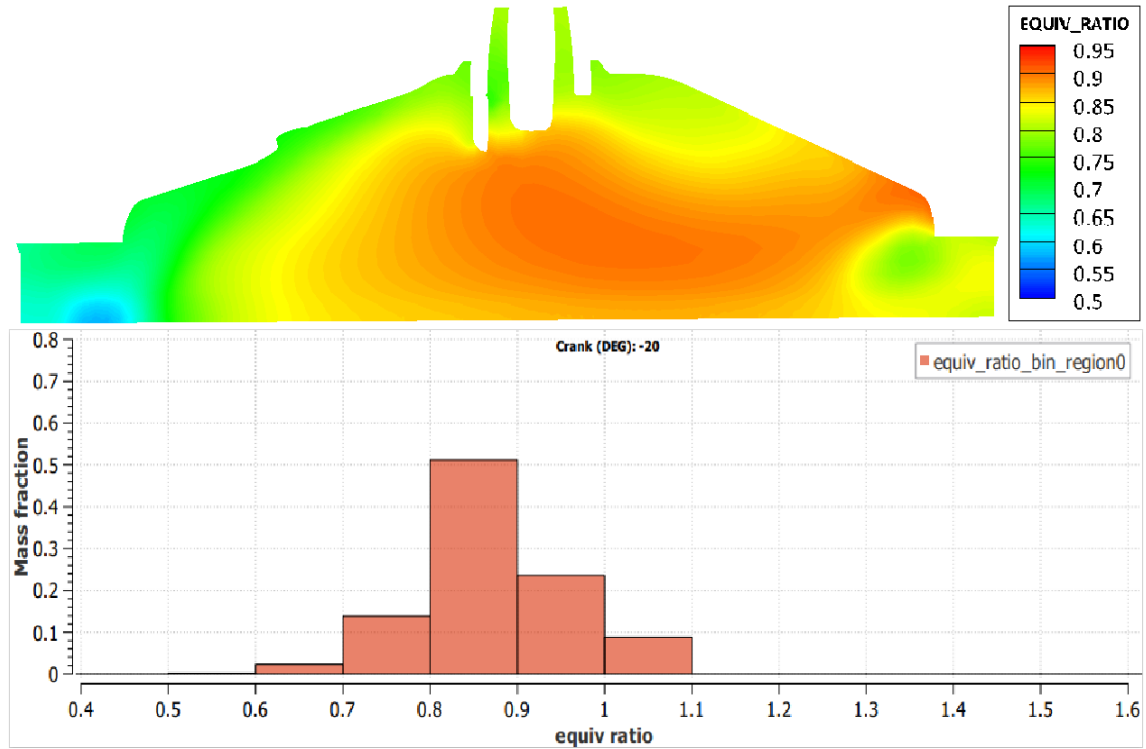


**Figure 3.23:** Equivalence ratio distribution for MCF with Piston temperature at 450K

Equivalence ratio distribution for MCF at  $T_w=450K$  In the figure [3.23] the two-dimensional slice of the cylinder shows the mixture to be stratified with multiple regions of colour with a rich mixture at the centre and leaner mixture on either sides and a very lean mixture (blue pocket) at the left bottom near the piston surface. This is confirmed by histogram, which shows a majority 50% of mixture between equivalence ratio of 0.8 and 0.9, 23% between 0.9 and 1.0, 13% between 0.7 and 0.8 and about 9% between 1.0 and 1.1 and the rest being very lean with ER around 0.6.

### 3.3.3.3 Fuel temperature = 363K

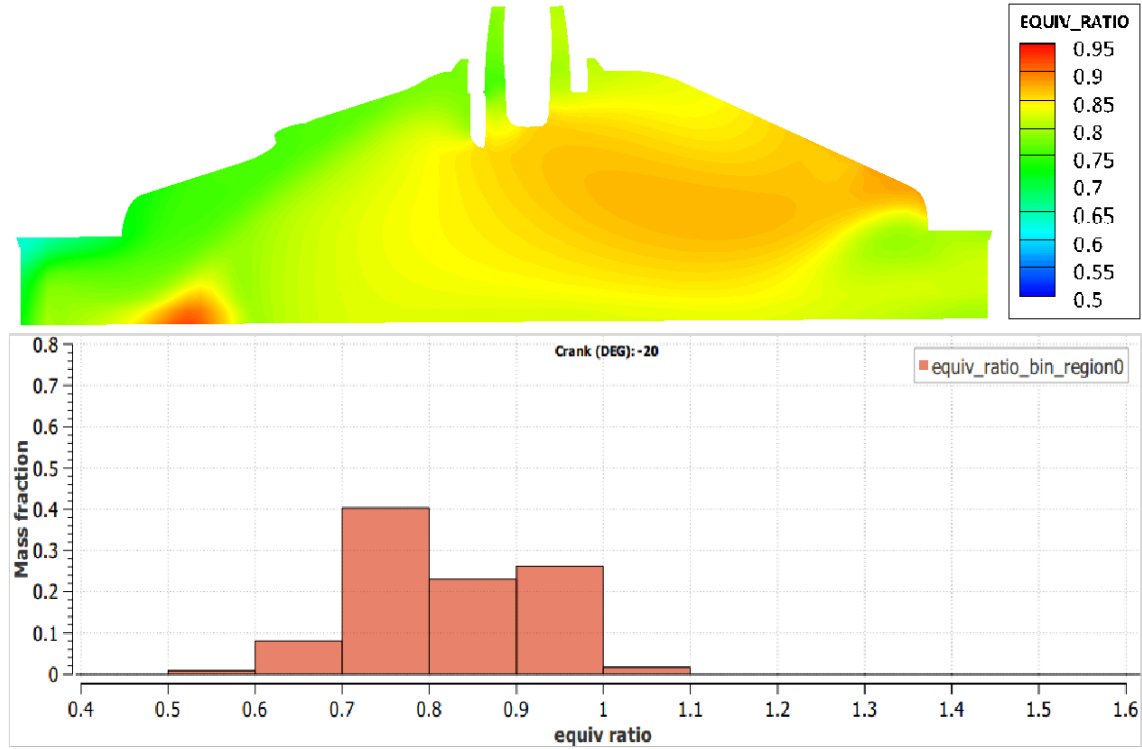


**Figure 3.24:** Equivalence ratio distribution for MCF with Fuel temperature at 363K

The image shows the existence of fuel rich mixture of equivalence ratio around 0.88 (Orange region) in the centre-right part of the cylinder surrounded by a region of mixture with ER around 0.85 (Yellow region). Leaner mixture pocket of ER 0.75 exists on the left side of the cylinder while the right side is comparatively has fuel rich mixture. Also, a fuel rich pocket of ER 1.0 near the piston on the left side, indicating the better homogeneous mixing on the right side but distinct pockets of different ER on the left side of the cylinder.

Histogram shows a total of 40% of mixture is at an equivalence ratio between 0.7 and 0.8, 26% between 0.9 and 1.0, 22% between 0.8 and 0.9, and majority of the rest of fuel being leaner with ER between 0.5 to 0.7. Considerably higher and equal percentage of air-fuel mixture spread across different ER bands and the presence of distinct leaner and richer pockets identifies the stratified nature of the charge in the cylinder which results in poor combustion compared to fuel temperature at 335K.



# 4

## Conclusion

- Higher piston and fuel temperatures result in less fuel film mass on the surface and faster evaporation.
- Lower fuel film mass on the piston and faster evaporation of the fuel results in better mixing, as it provides more time for evaporated fuel and the air to mix well.
- Multi-component fuel which has a realistic evaporation profile, provides better and more realistic results.
- Fuel back flow into the intake manifold was observed when the piston started moving from BDC to TDC.

#### 4. Conclusion

---

# 5

## Future work

As the CFD software takes the defined surface temperature to be constant throughout the surface, including a temporal and spatial temperature profile for the surfaces is beneficial for obtaining better and realistic results.

Changing the Start of Injection (SOI) to study its effects on fuel film mass, mixing and the fuel escape into the intake manifold. As the late injection might cause less fuel film mass on piston surface and earlier injection time more film.

Performing ignition in CFD simulations, with the optimal conditions based on the results of this thesis and study emissions.





# Bibliography

- [1] Köpple, F., Seboldt, D., Jochmann, P., Hettinger, A. et al., "Experimental Investigation of Fuel Impingement and Spray-Cooling on the Piston of a GDI Engine via Instantaneous Surface Temperature Measurements," SAE Int. J. Engines 7(3):2014, doi:10.4271/2014-01-1447
- [2] Richards, K. J., Senecal, P. K., and Pomraning, E., CONVERGE 3.0 Manual, Convergent Science, Madison, WI (2020).
- [3] Richards, K. J., Senecal, P. K., and Pomraning, E., CONVERGE 3.0, Convergent Science, Madison, WI (2020).
- [4] J.B. Heywood. Internal Combustion Engine Fundamentals. McGraw-Hill, 1988.
- [5] Köpple, F., Jochmann, P., Kufferath, A. and Bargende, M., "Investigation of the Parameters Influencing the Spray-Wall Interaction in a GDI Engine - Prerequisite for the Prediction of Particulate Emissions by Numerical Simulation," SAE Int. J. Engines 6(2):2013, doi:10.4271/2013-01-1089.





**CHALMERS**  
UNIVERSITY OF TECHNOLOGY